

Circuit Quantisation from First Principles

Yun-Chih Liao,^{1, 2,*} Ben J. Powell,² and Thomas M. Stace^{1, 2}

¹*ARC Centre of Excellence for Engineered Quantum Systems*

²*School of Mathematics and Physics, The University of Queensland, Brisbane, Queensland 4072, Australia*

Superconducting circuit quantisation conventionally starts from classical Euler-Lagrange circuit equations-of-motion. Invoking the correspondence principle yields a canonically quantised circuit description of circuit dynamics over a bosonic Hilbert space. This process has been very successful for describing experiments, but implicitly starts from the classical Ginsberg-Landau (GL) mean field theory for the circuit. Here we employ a different approach which starts from a microscopic fermionic Hamiltonian for interacting electrons, whose ground space is described by the Bardeen-Cooper-Schrieffer (BCS) many-body wavefunction that underpins conventional superconductivity. We introduce the BCS ground-space as a subspace of the full fermionic Hilbert space, and show that projecting the electronic Hamiltonian onto this subspace yields the standard Hamiltonian terms for Josephson junctions, capacitors and inductors, from which standard quantised circuit models follow. Importantly, this approach does not assume a spontaneously broken symmetry, which is important for quantised circuits that support superpositions of phases, and the phase-charge canonical commutation relations are derived from the underlying fermionic commutation properties, rather than imposed. By expanding the projective subspace, this approach can be extended to describe phenomena outside the BCS ground space, including quasiparticle excitations.

I. INTRODUCTION

Superconducting devices are one of the leading candidates for building quantum computers, showing great flexibility for implementing qubits and gates [1, 2]. The low working temperature reduces the noise, providing for long coherence time [3]. The strong coupling between superconducting qubits and electromagnetic fields allows us to control and operate the system [4].

The conventional approach to quantising superconducting circuits [5, 6] starts with the classical circuit equations of motion, which can be derived from the standard Kirchoff's laws, which are derived from a combination of conservation laws and the constitutive relations for specific elements that are present in the circuit. As long as the circuit is conservative, these equations are the Euler-Lagrange equations, which are generated from a Lagrangian. Canonical quantisation then proceeds, via the correspondence principle, by postulating commutation relations between classically conjugate coordinates describing the circuit phase space.

These classical equations describe the dynamics of the Ginsburg-Landau (GL) superconducting order parameters, ϕ_j , defined at the nodes j of the circuit. The GL order parameter is itself a classical mean field, approximating an underlying microscopic electronic Hamiltonian, and the (re-)quantisation procedure of the classical Euler-Lagrange equations for ϕ_j , described above, yields the standard bosonic theory for $\hat{\phi}_j$ with the conjugate coordinates being the circuit charges, \hat{n}_j .

This standard approach (vertical block sequence in fig. 1) is practically satisfactory for modelling the vast majority of experiments, however it is conceptually unfulfilling for several reasons. Firstly, we already have a very

successful microscopic quantum theory of superconductivity, namely, Bardeen-Cooper-Schrieffer (BCS) theory, which describes the dynamics of the microscopic electronic Hilbert space of interacting electrons in a metal. As such, there should be a “direct” pathway from the microscopic electronic Hamiltonian to the circuit Hamiltonian, without leaving the fermionic Hilbert space. In this goal, there is close analogy in modelling low-dimensional semiconducting systems (such as quantum dots [7] or quantum Hall fluids [8, 9]), in which a microscopic Fermi-liquid theory of semiconductors is projected onto a low-dimensional subspace of low-energy bound states in a spatially inhomogeneous, weakly-confining potential landscape, yielding effective descriptions in terms of mass-renormalised, few-electron (or hole) systems [8].

Secondly, the GL mean-field does not include phenomena such as quasiparticles or quantum fluctuations in the gap parameter, Δ , which are otherwise added ‘by-hand’ after re-quantisation [10, 11]. Thirdly, when re-quantising GL mean-field theory (MFT), bosonic canonical commutation relations are simply postulated from the classically-conjugate coordinates; in fact, we expect the correct commutation relations should emerge from the underlying fermionic degrees of freedom. Fourthly, GL mean-field theory assumes spontaneous symmetry breaking of the superconducting order parameter, however in the quantised circuit, we expect quantum superpositions of (relative) phases which is conceptually at odds with the notion of the spontaneous realisation of one (amongst the continuous manifold) of allowed phases.

Lastly, the classical GL MFT for the order parameter ϕ is indifferent to the support of ϕ : compact, $\phi \in [-\pi, \pi]$, and non-compact, $\phi \in \mathbb{R}$, descriptions of ϕ are entirely equivalent at a classical level. In contrast, the quantum descriptions of these two alternatives, or something in between, are not equivalent to one another [12]. Starting from the classical GL MFT therefore cannot resolve

* uqyliao1@uq.edu.au

which alternative provides the more accurate description.

The objective of this work is to provide a somewhat formal derivation of the Hamiltonian for superconducting circuits, starting from the microscopic theory of interacting electrons. To do this, we reformulate BCS theory slightly, by introducing a low energy Hilbert space of the set of BCS ground states, $\mathcal{H}_{\text{BCS}} = \text{span}\{|\Psi(\phi_j)\rangle\}_{\phi_j \in \mathcal{Z} \subset [-\pi, \pi]}$, where $|\Psi(\phi_j)\rangle$ is a BCS ground state (defined later), parameterised by a BCS phase angle ϕ_j . We define a projector, P onto \mathcal{H}_{BCS} , and use this projector to construct the low energy Hamiltonian (refer to the outer arrow in the flowchart fig. 1). We illustrate this approach for the conventional superconducting toolbox: capacitors, inductors, and Josephson junctions.

In subsequent sections we formalise this approach, and derive a number features of the model, including the discrete basis for \mathcal{H}_{BCS} , the commutation relations in the compact \mathcal{H}_{BCS} , and support for the low-energy Hilbert space of standard superconducting elements (inductors vs Josephson junctions). The new microscopic framework equips us with new insight of the matter phase and can be easily generalised to a bigger Hilbert space. With this approach, we develop the connection between superconducting BCS theory [13] and the well-known Cooper-pair-box (CPB) model [14].

This paper is organised as below: We firstly carry on the overlap of BCS states and discuss the requirements of discrete basis set constructed by them in Section II. In Section III, we project the LCJ circuit from the first principles and include the external field to the circuit. Finally we conclude the work and discuss the future outlook in Section V.

A. Microscopic Hamiltonian for Electrons

To introduce notation, we consider two pieces of superconducting metal separating by an insulator, which is equivalently an LCJ circuit shown in fig. 2. For the Josephson junction illustrated in fig. 2 (b), the superconducting islands A and B are described by their respective Hamiltonians [15],

$$H_{A,B} = H_{K_{A,B}} + H_{I_{A,B}}, \quad (1)$$

where the microscopic electron kinetic and interaction terms are given respectively in the momentum basis as

$$H_{K_A} = \sum_{\mathbf{k}_{A,S_A}} (\epsilon_{\mathbf{k}_A} - \mu_A) c_{\mathbf{k}_{A,S_A}}^\dagger c_{\mathbf{k}_{A,S_A}}, \quad (2)$$

$$H_{I_A} = -|g|^2 \sum_{\mathbf{k}_A \mathbf{k}'_A} c_{\mathbf{k}_A \uparrow}^\dagger c_{-\mathbf{k}_A \downarrow}^\dagger c_{-\mathbf{k}'_A \downarrow} c_{\mathbf{k}'_A \uparrow}, \quad (3)$$

and similarly for H_B .

Assuming point-like metallic islands, the Coulomb interaction between electrons on island A and B is given

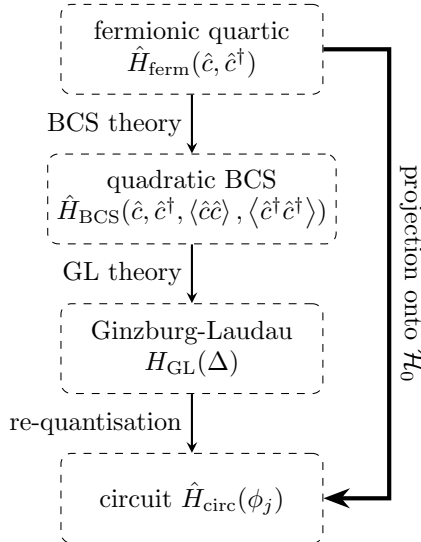


FIG. 1. The conventional approach to circuit quantisation (left pathway) conceptually begins with a microscopic electronic theory of interacting fermions in a metal, which proceeds to a classical Ginsburg-Landau mean-field theory (GL-MFT) of superconductivity in a metal, which is finally requantised to produce a quantised theory of a circuit. The approach described here (right pathway) starts at the same point, but uses the GL-MFT as inspiration to define a low-energy BCS subspace, \mathcal{H}_{BCS} (see eq. (10)) and then directly project the dynamics onto this subspace, resulting in the effective low-energy circuit Hamiltonian.

by

$$H_{\text{Coul}} = \lambda_C \sum_{\mathbf{k}_A \mathbf{k}_B s_A s_B} c_{\mathbf{k}_{A,S_A}}^\dagger c_{\mathbf{k}_{A,S_A}} c_{\mathbf{k}_{B,S_B}}^\dagger c_{\mathbf{k}_{B,S_B}}, \quad (4)$$

where $\lambda_C = \frac{1}{4\pi\epsilon} \frac{Q_A Q_B}{r^2}$ is the effective Coulomb interaction strength between the two point-like superconductor.

The electrons also tunnel between through the insulating barrier, with tunneling Hamiltonian

$$H_T = \sum_{\mathbf{k}_A \mathbf{k}_B s} t_{\mathbf{k}_A \mathbf{k}_B} c_{\mathbf{k}_A s}^\dagger c_{\mathbf{k}_B s} + t_{\mathbf{k}_A \mathbf{k}_B}^* c_{\mathbf{k}_B s}^\dagger c_{\mathbf{k}_A s}. \quad (5)$$

The parameters and the operators in the Hamiltonians are $\epsilon_{\mathbf{k}}$: the kinetic energy of the electron with momentum \mathbf{k} , μ : the chemical potential, g : the effective coupling strength between electrons, $t_{\mathbf{k}_A \mathbf{k}_B}$: tunneling matrix element depending on the initial and final states \mathbf{k}_A , \mathbf{k}_B respectively, and $c_{\mathbf{k}_l s_l}^\dagger$ and $c_{\mathbf{k}_l s_l}$: creation and annihilation operators for electron of momentum \mathbf{k}_l and spin s_l (index l labels the superconductor). The microscopic Hamiltonian for an electrical circuit including tunnel junctions is then $H_{\text{LCJ}} = H_A + H_B + H_{\text{Coul}} + H_T$.

Conventionally, the quartic Hamiltonian eq. (1) is solved approximately by factoring into a quadratic mean-

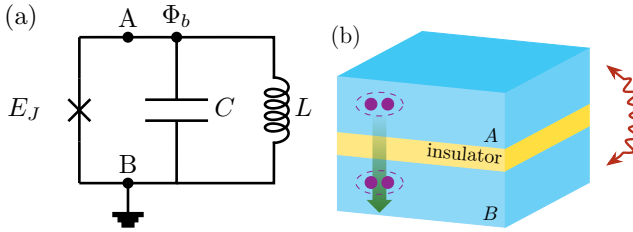


FIG. 2. (a) A standard LCJ circuit consists of a inductor L , a capacitor C , and a Josephson junction E_J made by superconductors. (b) A Josephson junction consists of two superconducting islands (blue) separated by an insulating tunnel barrier (yellow). At low temperature, the electrons bind into Cooper pairs which tunnel coherently across the (green arrow). In addition, the charges inside the two superconducting slabs have a capacitive Coulomb interaction (red arrow).

field theory, yielding

$$H_{\text{BCS}} = \sum_{\mathbf{k}s} (\epsilon_{\mathbf{k}} - \mu) c_{\mathbf{k}s}^\dagger c_{\mathbf{k}s} - |g|^2 \sum_{\mathbf{k}\mathbf{k}'} (\langle c_{\mathbf{k}\uparrow}^\dagger c_{-\mathbf{k}\downarrow}^\dagger \rangle c_{-\mathbf{k}\downarrow} c_{\mathbf{k}'\uparrow} + \text{h.c.}), \quad (6)$$

$$= \sum_{\mathbf{k}s} (\epsilon_{\mathbf{k}} - \mu) c_{\mathbf{k}s}^\dagger c_{\mathbf{k}s} - \sum_{\mathbf{k}} (\Delta^* c_{-\mathbf{k}\downarrow} c_{\mathbf{k}\uparrow} + \text{h.c.}). \quad (7)$$

where $\Delta = |g|^2 \sum_{\mathbf{k}} \langle c_{-\mathbf{k}\downarrow} c_{\mathbf{k}\uparrow} \rangle$ is the well-known complex superconducting order parameter. The quadratic Hamiltonian is diagonalised by the Bogoliubov-Valatin transformation to construct the BCS ground state

$$|\Psi(\Delta)\rangle = \prod_{\mathbf{k}} \left(u_{\mathbf{k}}(|\Delta|) + v_{\mathbf{k}}(|\Delta|) e^{i\arg(\Delta)} c_{\mathbf{k}\uparrow}^\dagger c_{-\mathbf{k}\downarrow}^\dagger \right) |0\rangle, \quad (8)$$

which is used to self-consistently solve for $|\Delta|$, and for which the phase $\phi \equiv \arg(\Delta)$ is a free classical coordinate.

We use this standard approach to motivate a choice of low energy basis states, but depart from it in that we do not impose the symmetry breaking implied by taking the partial expectations that transforms the microscopic quartic Hamiltonian into a quadratic form.

II. LOW-ENERGY BCS SUBSPACE

In this section, we use the well-known phase-symmetry-broken BCS ground state $|\Psi(\Delta)\rangle$ to motivate the introduction of a low-energy Hilbert space spanned by a set of equivalent BCS ground states $\{|\Psi(\phi)\rangle\}_{\phi \in [-\pi, \pi]}$.

We analyse the overlap of two BCS states from this set, and determine conditions for approximate basis orthogonality and completeness. We then construct ground-space phase and number operators, and connect the resulting phase-number commutator to the the now-venerable Pegg-Barnett theory [16].

A. BCS Ground Space

A ground state wavefunction of many paired electrons inside a superconductor is the BCS state [13]

$$|\Psi(\phi_j)\rangle = \prod_{\mathbf{k}} \left(u_{\mathbf{k}} + v_{\mathbf{k}} e^{i\phi_j} c_{\mathbf{k}\uparrow}^\dagger c_{-\mathbf{k}\downarrow}^\dagger \right) |0\rangle, \quad (9)$$

where $\phi_j \in [-\pi, \pi]$ is the phase of the superconductor, $u_{\mathbf{k}}, v_{\mathbf{k}}$ are variational parameters used to minimise the total energy, and $|0\rangle$ is the vacuum for electron Fock state.

We adopt the subscript j to preempt our intent to restrict the allowed phases to a discrete subset $\mathcal{Z} = \{\phi_j\}_{j \in \mathbb{Z}_{j_{\max}}}$. The core of our approach here is to define a basis of BCS ground states $\{|\Psi(\phi_j)\rangle\}_{\phi_j \in \mathcal{Z}}$ and the corresponding low-energy Hilbert space

$$\mathcal{H}_{\text{BCS}} = \text{span}\{|\Psi(\phi_j)\rangle\}_{\phi_j \in \mathcal{Z}}. \quad (10)$$

Projecting the microscopic electronic Hamiltonian into this subspace in which we (re)construct the low energy circuit theory without recourse to a re-quantisation procedure.

For a system consisting of multiple superconducting islands, the joint system forms a tensor product of the subsystems. For example the state of a system consisting of metallic islands A and B is spanned by the tensor product of single-island states as

$$\begin{aligned} |\Psi_{AB}(\phi_A, \phi_B)\rangle &= |\Psi_A(\phi_A)\rangle \otimes |\Psi_B(\phi_B)\rangle \\ &= \prod_{\mathbf{q}_A, \mathbf{q}_B} (u_{\mathbf{q}_A} + v_{\mathbf{q}_A} e^{i\phi_A} c_{\mathbf{k}_A\uparrow}^\dagger c_{-\mathbf{k}_A\downarrow}^\dagger) \\ &\quad \times (u_{\mathbf{q}_B} + v_{\mathbf{q}_B} e^{i\phi_B} c_{\mathbf{k}_B\uparrow}^\dagger c_{-\mathbf{k}_B\downarrow}^\dagger) |00\rangle, \\ &= \prod_{\mathbf{q}_A, \mathbf{q}_B} (u_{\mathbf{q}_A} + v_{\mathbf{q}_A} e^{i\phi_{AB}} c_{\mathbf{k}_A\uparrow}^\dagger c_{-\mathbf{k}_A\downarrow}^\dagger) \\ &\quad \times (u_{\mathbf{q}_B} + v_{\mathbf{q}_B} c_{\mathbf{k}_B\uparrow}^\dagger c_{-\mathbf{k}_B\downarrow}^\dagger) |00\rangle, \\ &= |\Psi_{AB}(\phi_{AB})\rangle, \end{aligned} \quad (11)$$

where a gauge transformation on the electronic operators allows us to express the joint state as a function of the relative phase between the two superconducting islands $\phi_{AB} \equiv \phi_A - \phi_B$.

B. BCS Ground-Space Projection Operator

This work is focussed on the dynamics of an electronic system restricted to the BCS ground space, so we define an (approximate) BCS ground space projection operator P onto \mathcal{H}_{BCS} [17] as

$$P = \sum_j |\Psi(\phi_j)\rangle \langle \Psi(\phi_j)|, \quad \bar{P} = \mathbb{I} - P, \quad (12)$$

where \mathbb{I} denotes the identity operator. The degree to which this is a well defined projector satisfying $P^2 = P$

depends on the orthogonality of the ground state basis, which we address below.

We will use the projection operator to construct effective operators acting on the low energy space. For example, a system of two superconducting islands with a microscopic electronic Hamiltonian $H_{\text{el}} = H_A + H_B + H_{\text{Coul}} + H_T$, the low-energy effective Hamiltonian is given by

$$PH_{\text{eff}}P \approx PH_0P + PH_1P + PH_1\bar{P}(\bar{P}E_0 - \bar{P}H_0\bar{P})^{-1}\bar{P}H_1P, \quad (13)$$

up to the second-order in the tunneling, where $H_0 = H_A + H_B + H_{\text{Coul}}$ and $H_1 = H_T$ is treated perturbatively.

C. BCS Subspace Orthogonality and Completeness

The overlap of BCS states in the basis with phases ϕ, ϕ' is given by the overlap function

$$\mathcal{W}(\varphi) \equiv \langle \Psi(\phi) | \Psi(\phi') \rangle = \prod_{\mathbf{k}} (u_{\mathbf{k}}^2 + v_{\mathbf{k}}^2 e^{i\varphi}), \quad (14)$$

where $\varphi \equiv \phi' - \phi$, the Bogoliubov coefficients are given by $u_{\mathbf{k}}^2 = (1 + (\epsilon_{\mathbf{k}} - \mu)/E_{\mathbf{k}})/2, v_{\mathbf{k}}^2 = (1 - (\epsilon_{\mathbf{k}} - \mu)/E_{\mathbf{k}})/2$ and we define $E_{\mathbf{k}} \equiv \sqrt{(\epsilon_{\mathbf{k}} - \mu)^2 + \Delta^2}$ [15].

We assume a half-filled electronic band consisting of $n \gg 1$ single particle modes with bandwidth $\pm \mathcal{B}$, so that $\epsilon_{\mathbf{k}} \in [-b\Delta, b\Delta]$, where $b = \mathcal{B}/\Delta$ is the dimensionless bandwidth in units of the gap. Typically $\mathcal{B} \sim 1\text{eV}$ [18] and $\Delta \sim 1\text{meV}$ [19], so $b \sim 1000 \gg 1$.

We take the logarithm of eq. (14) and write the momentum sum by an integral $\sum_{\mathbf{k}} \rightarrow 2 \int_0^{b\Delta} d\epsilon \rho(\epsilon)$, where the density of states is given by [20]

$$\rho(E_{\mathbf{k}}) = \frac{n}{2\Delta\sqrt{b^2 - 1}} \frac{E_{\mathbf{k}}}{\sqrt{E_{\mathbf{k}}^2 - \Delta^2}}, \quad (15)$$

to find

$$\begin{aligned} \ln(\mathcal{W}(\varphi)) &= \sum_{\mathbf{k}} \ln \left(\frac{1}{2} (1 + (\epsilon_{\mathbf{k}} - \mu)/E_{\mathbf{k}}) \right. \\ &\quad \left. + \frac{1}{2} e^{i\varphi} (1 - (\epsilon_{\mathbf{k}} - \mu)/E_{\mathbf{k}}) \right), \\ &= 2 \int_0^{b\Delta} d\epsilon \rho(\epsilon) \ln \left(\frac{1}{2} (1 + (\epsilon_{\mathbf{k}} - \mu)/E_{\mathbf{k}}) \right. \\ &\quad \left. + \frac{1}{2} e^{i\varphi} (1 - (\epsilon_{\mathbf{k}} - \mu)/E_{\mathbf{k}}) \right), \\ &\approx n \left(i \frac{1 + b - \sqrt{b^2 - 1}}{4(b + 1)} \varphi \right. \\ &\quad \left. - \frac{\pi - 4 \arctan(b - \sqrt{b^2 - 1})}{32\sqrt{b^2 - 1}} \varphi^2 \right), \\ &= n(i\varphi/4 - \pi\varphi^2/32)/b + O(1/b^2). \end{aligned} \quad (16)$$

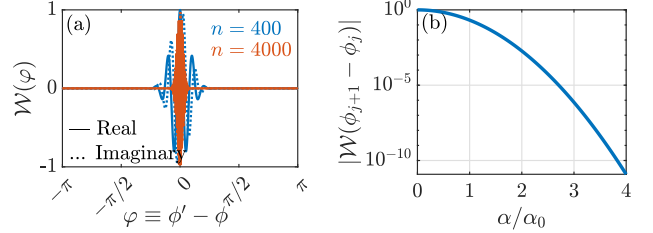


FIG. 3. (a) Overlap of the BCS states $\mathcal{W}(\varphi) = \langle \Psi(\phi) | \Psi(\phi') \rangle$ as a function of the phase difference $\varphi \equiv \phi' - \phi$. Increasing the number of electron modes, n , leads to faster oscillations over a narrower range, and the overlap $\mathcal{W}(\varphi)$ tends to a pseudo-Kronecker delta function, $\mathcal{W}(\phi_j - \phi_{j'}) \xrightarrow{n \rightarrow \infty} \delta_{j,j'}$. For this plot we have set $b = 10$. (b) The overlap amplitude of adjacent basis states eq. (20) As α grows, neighbouring phase states become increasingly orthogonal.

It follows that

$$\mathcal{W}(\varphi) \approx e^{n(i\varphi/4 - \pi\varphi^2/32)/b}, \quad (17)$$

so that the overlap is approximately a Gaussian envelope of width $\sim \sqrt{b/n}$, modulated by an oscillating function. We plot $\mathcal{W}(\varphi)$ in fig. 3(a), showing both the state normalisation condition $\mathcal{W}(0) = 1$, and that \mathcal{W} decreases quickly for $\varphi > \sqrt{b/n}$.

We now use the functional form of \mathcal{W} to establish conditions under which we can construct an approximately orthogonal basis of phase states which is also complete in the low-energy subspace.

1. Basis Orthogonality

An orthogonal basis of phase states would satisfy $\mathcal{W}(\phi' - \phi) = 0, \forall \phi \neq \phi'$. However, $|\mathcal{W}(\phi' - \phi)| > 1$, and so any set $\{|\Psi(\phi)\rangle\}$ is not precisely orthogonal. Nonetheless fig. 3a shows that $\mathcal{W}(\varphi)$ is a rapidly decreasing function of $|\varphi|$, and so we construct an approximately orthogonal basis by discretising $\phi \in [-\pi, \pi]$ with discretisation interval $\delta\phi = \phi_{j+1} - \phi_j$, to construct the discrete set of phases $\phi_j = -\pi + \delta\phi \cdot j$ with $j \in \mathbb{Z}_{j_{\text{max}}} \equiv \{0, 1, \dots, j_{\text{max}} = \lfloor 2\pi/\delta\phi \rfloor\}$, so that

$$\phi_j \in \mathcal{Z} = 2\pi(\mathbb{Z}_{j_{\text{max}}} / j_{\text{max}} - 1/2) \subset [-\pi, \pi]. \quad (18)$$

From eq. (17), the overlap amplitude of neighbouring basis states is given by

$$|\mathcal{W}(\delta\phi)| = e^{-\delta\phi^2 n \pi / (32b)}. \quad (19)$$

We choose $\delta\phi = 2\pi\alpha/\sqrt{n}$ where α is a parameter controlling the overlap, so that

$$|\mathcal{W}(\delta\phi)| \approx e^{-\pi^3 \alpha^2 / (8b)} = e^{-\pi \alpha^2 / (2\alpha_0^2)} \quad (20)$$

is independent of the electron number, and we define $\alpha_0 = 2\sqrt{b}/\pi$. With the choice of $\delta\phi$ above, the dimension

of the BCS subspace basis is $j_{\max} = \sqrt{n}/\alpha$. This has the effects that the phase states become increasingly dense in the interval $[-\pi, \pi]$ as n grows, and that $j_{\max} \ll n$, so that the effective dimension of the BCS subspace is much smaller than the number of single-particle modes.

The parameter α determines how close to orthogonality the basis choice is, and should give

$$\langle \Psi(\phi_j) | \Psi(\phi_{j'}) \rangle \approx \delta_{j,j'}. \quad (21)$$

The plot in fig. 3b shows that choosing $\alpha \gtrsim 2\alpha_0$ produces a nearly orthogonal basis with $|\mathcal{W}(\delta\phi)| < e^{-2\pi} \sim 10^{-3}$.

2. Basis Completeness

Given a discrete set of phases $\phi_{j \in \mathcal{Z}}$, we cannot perfectly represent an arbitrary state $|\Psi(\phi)\rangle$ where $\phi \notin \phi_{j \in \mathcal{Z}}$. Here we analyse how well the Hilbert space $\mathcal{H}_{\text{BCS}} = \text{span}\{|\Psi(\phi_j)\rangle\}_{j \in \mathcal{Z}}$ covers all possible phase states $|\Psi(\phi)\rangle$ by bounding the distance d between $|\Psi(\phi)\rangle$ and \mathcal{H}_{BCS} . We find

$$\begin{aligned} d(|\Psi(\phi)\rangle, \mathcal{H}_{\text{BCS}}) &= \min_{\{a_j\}} d(|\Psi(\phi)\rangle, \sum_j a_j |\Psi(\phi_j)\rangle), \\ &= \min_{\{a_j\}} \left| |\Psi(\phi)\rangle - \sum_j a_j |\Psi(\phi_j)\rangle \right|, \\ &\leq \min_{\{a_j\}} 2 \left(1 - \sum_j a_j |\mathcal{W}(\phi_j - \phi)| \right), \\ &\leq 2 \min_j (1 - |\mathcal{W}(\phi_j - \phi)|), \\ &\leq 2(1 - |\mathcal{W}(\delta\phi)|), \\ &\approx 2(1 - e^{-\pi\alpha^2/(2\alpha_0^2)}). \end{aligned} \quad (22)$$

Smaller values for the upper estimate of d implies a more complete basis, capable of representing a larger set of phases. This suggests that small values of α are preferred. This is contrary to the requirement of basis orthogonality, which favours larger α . There is therefore a trade-off between orthogonality of the basis and completeness of representation.

3. Projection Error

The competing factors in control parameter α are orthogonality and completeness of the basis set. Here we synthesise both factors by computing the projection error for arbitrary phase states onto the low energy BCS subspace. We quantify the degree to which the discretised subspace \mathcal{H}_{BCS} can represent an arbitrary phase state $|\Psi(\phi)\rangle$, by computing its projection onto \mathcal{H}_{BCS}

$$K_n(\phi) \equiv \langle \Psi(\phi) | P | \Psi(\phi) \rangle = \sum_{\phi_j \in \mathcal{Z}} |\mathcal{W}(\phi - \phi_j)|^2. \quad (23)$$

This quantity is oscillatory, with maxima when $\phi \in \{\phi_j\}$, and minima when $\phi = (\phi_j + \phi_{j+1})/2$, and is plotted in fig. 4 for $\alpha = \alpha_0$ and $2\alpha_0$. The mean of the oscillatory

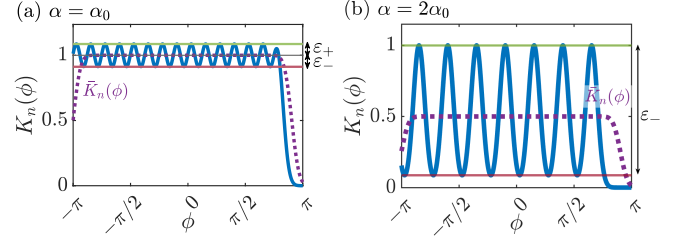


FIG. 4. Projections eq. (23) (blue solid lines) and their integral approximations eq. (24) for (a) $\alpha = \alpha_0$, in which the approximate BCS projection is close to unity everywhere but has normalisation errors with $K_n > 1$, and (b) $\alpha = 2\alpha_0$ where the normalisation error is negligible, but with poorly represented states at $\phi = (\phi_{j+1} - \phi_j)/2$. The parameters are chosen to be $n = 10^3$, $b = 10$ here.

projection is approximated by turning the sum into an integral,

$$\begin{aligned} \bar{K}_n(\phi) &= \int_0^{\sqrt{n-1}/\alpha} dj e^{-n(\phi - \pi + \frac{2\pi\alpha j}{\sqrt{n}})^2/(4\alpha_0^2)}, \\ &\approx \frac{\alpha_0}{2\alpha} \text{erf} \left[\frac{(\pi - \phi)\sqrt{n}}{\alpha_0\sqrt{\pi}} \right] \left(1 - \text{erf} \left[\frac{-2\pi\sqrt{n-1}}{\alpha_0\sqrt{\pi}} \right] \right), \end{aligned} \quad (24)$$

which interpolates between the maxima and minima of K . The integral approximation \bar{K} is also shown in fig. 4. For small α , $K \sim 1$ everywhere indicating that it can well represent arbitrary phase states, however, $K > 1$ for some values of ϕ indicating that it is not well normalised. Conversely, for larger α , the minima in K are much lower than unity, indicating that the subspace cannot well represent arbitrary phase states. The maxima and minima of K reflect the tradeoff between completeness and orthogonality, described above. We conclude that $\alpha \sim 2\alpha_0$ is a reasonable tradeoff between completeness and orthogonality. For metallic islands that lie at the boundary of microscopic and mesoscopic devices, there may be physical effects arising from small n effects, but do not pursue this analysis any further here.

D. Phase and Charge Operators

Having constructed a formal low energy Hilbert space from a discrete basis of phase states, in this section we define a basis of “number” states through a Fourier transformation. These two bases implicitly define the low-energy phase and charge operators, $\hat{\phi}$ and \hat{N} , and from these we compute commutation relations.

The BCS states $|\Psi(\phi_j)\rangle$ are not eigenstates of the electron number. Here we define low-energy “charge” eigenstates $|\Psi(N)\rangle$ via a discrete Fourier transform

$$|\Psi(N)\rangle \equiv \left(\frac{\alpha}{\sqrt{n-1} + \alpha} \right)^{1/2} \sum_{\phi_j} e^{-iN\phi_j} |\Psi(\phi_j)\rangle, \quad (25)$$

where the prefactor ensures normalisation.

We show in appendix A that $|\Psi(N)\rangle$ are eigenstates of the microscopic Cooper pair number operator $\hat{N}_{\text{CP}} = \sum_{\mathbf{k}} (c_{\mathbf{k}\uparrow}^\dagger c_{\mathbf{k}\uparrow} + c_{-\mathbf{k}\downarrow}^\dagger c_{-\mathbf{k}\downarrow})/2$, i.e.

$$\hat{N}_{\text{CP}} |\Psi(N)\rangle = N |\Psi(N)\rangle, \quad (26)$$

establishing that the Fourier conjugate states are indeed charge-number eigenstates, and the set $\{|\Psi(N)\rangle\}$, defines a conjugate charge-number basis. The charge-number has to be a positive integer within the range $[\frac{n}{2} - \frac{j_{\max}}{2}, \frac{n}{2} + \frac{j_{\max}}{2}]$ because the electron band is half-occupied. From here we can represent the Cooper pair number operator

with the number basis:

$$\hat{N} = \sum_{N=\frac{n}{2}-\frac{j_{\max}}{2}}^{\frac{n}{2}+\frac{j_{\max}}{2}} N |\Psi(N)\rangle \langle \Psi(N)|. \quad (27)$$

It is known that in optical systems, the phase-number commutator follows the commutator-Poisson-bracket correspondence for physical states [16]. In the following we aim to explore the canonical relation between the matter phase operator $\hat{\phi}$ and Cooper pair number operator \hat{N} in a single superconducting island, and generalise to the joined system consisting of two superconductors.

We represent the phase operator $\hat{\phi}$ in the number basis $\{|\Psi(N)\rangle\}$:

$$\begin{aligned} \hat{\phi} &\equiv \sum_{j=0}^{j_{\max}} \phi_j |\Psi(\phi_j)\rangle \langle \Psi(\phi_j)|, \\ &= \phi_0 \mathbb{I} + \frac{2\pi\alpha}{\sqrt{n}} \sum_{j=0}^{j_{\max}} \frac{j}{\sqrt{n-1} + \alpha} \sum_{NN'} e^{i(N-N')(\phi_0 + \frac{2\pi\alpha}{\sqrt{n}} j)} |\Psi(N)\rangle \langle \Psi(N')|, \\ &= \left(\phi_0 + \frac{\pi\alpha}{\sqrt{n}} \right) \mathbb{I} + \frac{2\pi\alpha}{\sqrt{n}} \frac{\sqrt{n-1}}{\sqrt{n-1} + \alpha} \sum_{N \neq N'} e^{i\phi_0(N-N')} \frac{e^{2\pi i \alpha(N-N')/\sqrt{n-1}}}{e^{2\pi i \alpha(N-N')/\sqrt{n-1}} - 1} |\Psi(N)\rangle \langle \Psi(N')|, \end{aligned} \quad (28)$$

where ϕ_0 denotes the reference phase attaching to the superconductor's phase. With the use of eq. (28), the phase-number commutator in the number representation can be computed. In the limit of $n \gg N, N'$, the commutator has the matrix elements

$$\langle \Psi(N) | [\hat{\phi}, \hat{N}] | \Psi(N') \rangle = \begin{cases} 0, & N = N' \\ \frac{2\pi\alpha\sqrt{n-1}}{\sqrt{n}(\sqrt{n-1} + \alpha)} (N' - N) e^{i\phi_0(N-N')} \frac{e^{2\pi i \alpha(N-N')/\sqrt{n-1}}}{e^{2\pi i \alpha(N-N')/\sqrt{n-1}} - 1}, & N \neq N' \end{cases} \quad (29)$$

The commutator is traceless as the diagonal element of $\hat{\phi}$ in N -representation is constant. For a system including numerous electrons $n \rightarrow \infty$, eq. (29) reduces to

$$\langle \Psi(N) | [\hat{\phi}, \hat{N}] | \Psi(N') \rangle \approx i (1 - \delta_{NN'}) e^{i\phi_0(N-N')}. \quad (30)$$

The approximate equality becomes exact when $n \rightarrow \infty$. The second term in eq. (30) is described in Pegg-Barnett analogue [16]. Transforming back to the ϕ representation, the commutator becomes

$$[\hat{\phi}, \hat{N}] \approx -i \left(\mathbb{I} - \frac{\sqrt{n-1} + \alpha}{\alpha} |\Psi(\phi_0)\rangle \langle \Psi(\phi_0)| \right). \quad (31)$$

Therefore, the expectation value of the commutator with respect to an arbitrary phase state $|\Psi(\phi)\rangle$ is given by

$$\begin{aligned} \langle \Psi(\phi) | [\hat{\phi}, \hat{N}] | \Psi(\phi) \rangle &\approx -i \left(1 - \frac{\sqrt{n-1} + \alpha}{\alpha} |J(\phi_0 - \phi)|^2 \right), \\ &\approx -i \left(1 - \frac{2\pi}{\delta\phi} \delta_{\phi_0, \phi} \right). \end{aligned} \quad (32)$$

We use $(\sqrt{n-1} + \alpha)/\alpha \approx 2\pi/(\delta\phi)$ for large $n \gg \alpha$, where $\delta\phi \equiv \phi_{j+1} - \phi_j$ is the spacing between adjacent phases. Thus, $\frac{\delta_{\phi_0, \phi}}{\delta\phi} \sim \delta(\phi_0 - \phi)$. We therefore obtain the minimum uncertainty measurement in an arbitrary phase state for a single superconductor:

$$(\Delta N)(\Delta\phi) \gtrsim \frac{1}{2} (1 - 2\pi\delta(\phi_0 - \phi)). \quad (33)$$

The factor 2π maintains the phase eigenvalues for the chosen 2π range and takes care of the periodic nature of phase.

In joined systems containing more than one superconductor, such as Josephson junctions, we are interested in the commutator of the phase and number difference between two islands. Assuming the junction is symmetric such that $n_A \approx n_B \equiv n$ and $\alpha_A \approx \alpha_B \equiv \alpha$, we have

$$[\hat{\phi}_{AB}, \hat{N}_{AB}] \equiv [\hat{\phi}_A - \hat{\phi}_B, \hat{N}_A - \hat{N}_B], \quad (34a)$$

$$\approx -2i(\mathbb{I}_A \otimes \mathbb{I}_B) + i \frac{\sqrt{n-1} + \alpha}{\alpha} \left(\left| \Psi_A(\phi_0^{(A)}) \right\rangle \left\langle \Psi_A(\phi_0^{(A)}) \right| \otimes \mathbb{I}_B + \mathbb{I}_A \otimes \left| \Psi_B(\phi_0^{(B)}) \right\rangle \left\langle \Psi_B(\phi_0^{(B)}) \right| \right). \quad (34b)$$

The basis states of the system is now a tensor state, depending on the phase difference: $|\Psi(\phi_{AB})\rangle = |\Psi_A(\phi_A)\rangle \otimes |\Psi_B(\phi_B)\rangle$. With reference phase difference defined by $\phi_0 \equiv \phi_0^{(A)} - \phi_0^{(B)}$, we obtain the expectation value

$$\begin{aligned} \langle \Psi(\phi_{AB}) | [\hat{\phi}_{AB}, \hat{N}_{AB}] | \Psi(\phi_{AB}) \rangle \\ \approx -2i \left(1 - \frac{2\pi}{\delta\phi} \cdot \delta_{\phi_0, \phi_{AB}} \right), \end{aligned} \quad (35)$$

such that the number-phase uncertainty relation of a Josephson junction is given by

$$(\Delta N_{AB})(\Delta \phi_{AB}) \gtrsim 1 - 2\pi\delta(\phi_0 - \phi_{AB}), \quad (36)$$

i.e., twice of that of a single superconductor.

In this subsection, we construct the canonical relation in the low-energy subspace for a system consisting of a Josephson junction, and shows that the Cooper pair number and the matter phase are the conjugate variable to each other.

III. PROJECTION OF LCJ CIRCUIT

As the low-energy Hilbert space \mathcal{H}_0 is constructed, we can derive the effective Hamiltonian from the first principles. With the use of the projection operator method given in eq. (13), we evaluate the effective Hamiltonian of the LCJ circuit in \mathcal{H}_0 up to the second-order in electron tunneling. By comparing the result with the conventional Cooper-pair-box model, we shall be able to establish the connection between the microscopic and macroscopic pictures.

According to perturbation theory, the zeroth-order term is the projection of the unperturbed Hamiltonian:

$$PH_0P = PH_AP + PH_BP + PH_{\text{Coul}}P. \quad (37)$$

Below we evaluate the superconducting island term and the Coulomb interaction separately.

A. Island Terms

We analyse the projections of the island Hamiltonian eq. (1),

$$PH_{A,B}P = \sum_{jj'} \langle \Psi(\phi_j) | H_{A,B} | \Psi(\phi_{j'}) \rangle | \Psi(\phi_j) \rangle \langle \Psi(\phi_{j'}) |,$$

here. Considering the superconducting metal A , the projection onto the low-energy subspace is given by

$$PH_AP = \sum_{jj'} \left\{ 2 \sum_{\mathbf{k}_A} \frac{(\epsilon_{\mathbf{k}_A} - \mu_l) v_{\mathbf{k}_A}^2}{u_{\mathbf{k}_A}^2 + v_{\mathbf{k}_A}^2 e^{i(\phi_{j'} - \phi_j)}} - |g|^2 \left(\sum_{\mathbf{k}_A} \frac{u_{\mathbf{k}_A} v_{\mathbf{k}_A}}{u_{\mathbf{k}_A}^2 + v_{\mathbf{k}_A}^2 e^{i(\phi_{j'} - \phi_j)}} \right)^2 \right\} e^{i(\phi_{j'} - \phi_j)} \langle \Psi(\phi_j) | \Psi(\phi_{j'}) \rangle | \Psi(\phi_j) \rangle \langle \Psi(\phi_{j'}) |, \quad (38)$$

whose matrix elements depend only on the phase difference $\varphi = \phi_{j'} - \phi_j$. By expressing $u_{\mathbf{k}}$ and $v_{\mathbf{k}}$ in terms of Δ , $E_{\mathbf{k}}$ [15] and replacing the momentum sum by the energy integral, $\sum_{\mathbf{k}=-\infty}^{\infty} \rightarrow \int_{\Delta}^{b\Delta} dE \rho(E)$, the matrix elements

are

$$\langle \Psi(\phi_j) | H_A | \Psi(\phi_{j'}) \rangle = \mathcal{K}(\varphi) - |g|^2 \mathcal{V}(\varphi), \quad (39)$$

where $\varphi \equiv \phi_{j'} - \phi_j$. The complex functions $\mathcal{K}(\varphi)$, $\mathcal{V}(\varphi)$ and the calculation detail are given in appendix B. We reduce the projection to

$$PH_A P = \sum_{jj'} \left(2\mathcal{K}(\varphi_{jj'}) - |g|^2 \mathcal{V}(\varphi_{jj'}) \right) e^{i\varphi_{jj'}} \mathcal{W}(\varphi_{jj'}) |\Psi(\phi_j)\rangle\langle\Psi(\phi_{j'})|, \quad \varphi_{jj'} = \phi_{j'} - \phi_j. \quad (40)$$

fig. 5 (a) and (b) shows the real and imaginary parts of the matrix element $(2\mathcal{K}(\varphi) - |g|^2 \mathcal{V}(\varphi)) e^{i\varphi} \mathcal{W}(\varphi)$. The function behaves similarly to $J(\varphi)$, who has maximum at $\varphi = 0$ and drops to zero dramatically for $\varphi \neq 0$ as $n \rightarrow \infty$. The diagonal elements of $PH_A P$ whose $\varphi = 0$ gives the mean ground-state energy:

$$\begin{aligned} \langle \Psi(\phi) | H_A | \Psi(\phi) \rangle &= 2\mathcal{K}(0) - |g_A|^2 \mathcal{V}(0), \\ &= \frac{-n_A \Delta_A^2}{4\mathcal{B}_A^2} \left[\mathcal{B}_A + 2\mathcal{B}_A \ln \frac{\Delta_A}{2\mathcal{B}_A} + |g_A|^2 n_A \ln \left(\frac{\Delta_A}{2\mathcal{B}_A} \right)^2 \right] + \mathcal{O}\left(\frac{1}{b_A^2}\right), \quad \mathcal{B}_A \equiv b_A \Delta_A \end{aligned} \quad (41a)$$

$$\equiv E_A(\mathcal{B}_A, \Delta_A), \quad (41b)$$

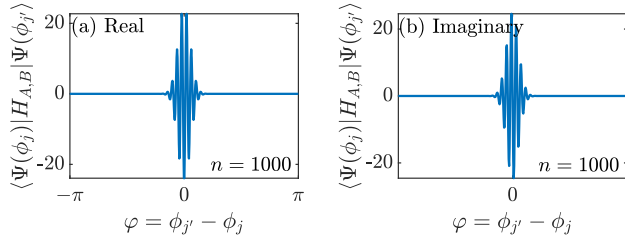


FIG. 5. Matrix element $\langle \Psi(\phi_j) | H_{A,B} | \Psi(\phi_{j'}) \rangle$ for $n = 10^3$, $\Delta = 1$, $b = 10$ case. The real and imaginary parts are illustrated in subfigure (a) and (b), respectively.

which depends on the gap and electron bandwidth of the material. Similarly, we obtain $E_B(\mathcal{B}_B, \Delta_B)$ for the metal B . The energy eq. (41) is the Higgs modes of the superconductor and will be further discussed in section IV B.

1. Minimum Energy of the Superconducting Island

We have calculated the eigenenergy of the superconducting island $E_A(\mathcal{B}_A, \Delta_A)$ as a function of bandwidth and gap in eq. (41). This energy has the minimum E_A^{\min} at $\Delta_A = \Delta_A^{\min}$ where $\frac{\partial E_A}{\partial \Delta}|_{\Delta_A=\Delta_A^{\min}} = 0$. Following Ref. [15] we define the electron-phonon coupling constant by

$$\lambda_A \equiv |g_A|^2 \rho(E_F) \approx \frac{|g_A|^2 n_A}{2\mathcal{B}_A}, \quad (42)$$

and obtain

$$\Delta_A^{\min} = 2\mathcal{B}_A e^{-1/\lambda_A}, \quad (43a)$$

$$E_A^{\min} = -\mathcal{B}_A e^{-2/\lambda_A} n_A. \quad (43b)$$

In mean-field theory, the system will relax to $\Delta_A = \Delta_A^{\min}$ [15]. The zero energy is set to be the Fermi level of the superconductor.

With the orthogonality of the BCS basis states discussed in section II C 1, the overlap of two BCS states

$\mathcal{W}(\varphi) \sim 1/\sqrt{n}$ and $\mathcal{W}(\varphi) \rightarrow \delta_{jj'}$ when $n \rightarrow \infty$, the projection of the individual superconductor reads

$$PH_A P = E_A P, \quad PH_B P = E_B P. \quad (44)$$

At absolute zero, $E_A \approx E_A^{\min}$, $E_B \approx E_B^{\min}$ are the ground-state energy of the individual islands.

B. Capacitance: Coulomb Interactions

The other component of the projection of the unperturbed Hamiltonian is the Coulomb interactions. The projection,

$$PH_{\text{Coul}} P = \sum_{jj'} \langle \Psi(\phi_j) | H_{\text{Coul}} | \Psi(\phi_{j'}) \rangle | \Psi(\phi_j) \rangle \langle \Psi(\phi_{j'}) |, \quad (45)$$

has matrix elements

$$\begin{aligned} \langle \Psi(\phi_j) | H_{\text{Coul}} | \Psi(\phi_{j'}) \rangle &= 4\lambda_C \sum_{\mathbf{k}_A \mathbf{k}_B} \frac{v_{\mathbf{k}_A}^2 v_{\mathbf{k}_B}^2 e^{i(\phi_{j'} - \phi_j)}}{u_{\mathbf{k}_A}^2 + v_{\mathbf{k}_A}^2 e^{i(\phi_{j'} - \phi_j)}} \\ &\times \langle \Psi(\phi_j) | \Psi(\phi_{j'}) \rangle, \end{aligned} \quad (46)$$

and relates to the electron number of the superconducting islands. Given $\hat{N} |\Psi(N)\rangle = N |\Psi(N)\rangle$, where $|\Psi(N)\rangle$ is the number state (details are in appendix A), H_{Coul} in number-representation reads

$$H_{\text{Coul}} = \lambda_C \hat{N}_A^e \hat{N}_B^e = 4\lambda_C \hat{N}_A \hat{N}_B, \quad (47)$$

where $\hat{N}^e = 2\hat{N}$ is the electron number operator. With $P |\Psi(N_A, N_B)\rangle = |\Psi(N_A, N_B)\rangle$, eventually we obtain the projection of Coulomb Hamiltonian:

$$PH_{\text{Coul}} P = 4\lambda_C \hat{N}_A \hat{N}_B. \quad (48)$$

This term relates to the capacitance energy of the circuit as $\hat{N}_A \hat{N}_B \propto Q_A Q_B$, the product of the charge on the two slabs. Hence the capacitance energy of the circuit is the Coulomb interaction between the two superconductors.

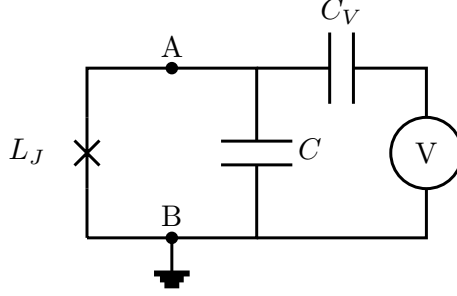


FIG. 6. A circuit consisting of a Josephson junction with a bias voltage V connected capacitively. The bias voltage creates an offset charge n_g to the capacitance Hamiltonian.

Combining the results in Eqs. (44), (47), the zeroth-order term in tunneling reads

$$PH_0P \approx 4\lambda\hat{N}_A\hat{N}_B + (E_A + E_B)P, \quad (48)$$

where E_A , E_B are the ground-state energies of the superconductors, which depends on the temperature. In the zero-temperature limit, E_A , E_B are the minimised energies given in eq. (43b).

Non-zero bias: Consider a bias charge $n_g \neq 0$, fig. 6. The total charge carriers on the both islands are sifted: $N_A \rightarrow N'_A = N_A + n_e$, $N_B \rightarrow$

$N'_B = N_B - n_e$, where $n_e = CV/(2e)$. The effective charge on the capacitor $N'_{AB} = N'_A - N'_B$ becomes $N_{\text{tot}}^2 - 4(N_AN_B - n_e^2 - n_e(N_A - N_B))$. From the conservation of the total charge $N'_{\text{tot}} = N_{\text{tot}}$, we obtain

$$(N'_{AB} - (2n_e))^2 = -4N_AN_B + N_{\text{tot}}^2. \quad (49)$$

The offset charge $n_g = 2n_e$, results from the electron pairing in superconductors. In summary, the capacitance term in eq. (47) shifts for a non-zero charge bias.

C. Josephson Effect: Second-Order Tunneling

First-order in tunneling: The first-order tunneling term is given by $PH_T P$ [17]. The mechanism of H_T , who shifts one electron from one side to the other side. This changes the parity of the wavefunction on the two sides of the junction. As the wavefunctions are orthogonal for even and odd number states, the matrix element vanishes: $\langle \Psi(\phi_j) | H_T | \Psi(\phi_{j'}) \rangle = 0$. Therefore, the first-order term in tunneling is zero,

$$PH_T P = 0. \quad (50)$$

The projection of the second-order term in tunneling is given by

$$PH_T(E_0\bar{P} - \bar{P}H_0\bar{P})^{-1}H_T P = \sum_{jj'} \langle \Psi(\phi_j) | H_T(E_0\bar{P} - \bar{P}H_0\bar{P})^{-1}H_T | \Psi(\phi_{j'}) \rangle | \Psi(\phi_j) \rangle \langle \Psi(\phi_{j'}) |.$$

The matrix elements can be evaluated from the Fourier's transform of the Greens' functions if $j = j'$ (i.e., the diagonal elements) [21]:

$$\begin{aligned} \langle \Psi(\phi_j) | H_T(E_0\bar{P} - \bar{P}H_0\bar{P})^{-1}H_T | \Psi(\phi_j) \rangle \\ = \mathcal{F}_{\tau \rightarrow E_0} \langle \mathcal{T}_\tau [H_T(\tau)H_T] \rangle. \end{aligned} \quad (51)$$

A similar calculation of the Josephson tunneling yields

$$\begin{aligned} \langle \Psi(\phi_j) | H_T(E_0\bar{P} - \bar{P}H_0\bar{P})^{-1}H_T | \Psi(\phi_j) \rangle \\ = 2 \sum_{\mathbf{k}_A \mathbf{k}_B} t^2 e^{i\phi_j} \mathcal{F}_{\uparrow\downarrow}(\mathbf{k}_A, \tau) \mathcal{F}_{\downarrow\uparrow}(\mathbf{k}_B, \tau) + \text{c.c.}, \end{aligned}$$

where t is the constant tunneling matrix element, and $\mathcal{F}_{\uparrow\downarrow}$ and $\mathcal{F}_{\downarrow\uparrow}$ are anomalous Green's functions in reciprocal space, defined by $\mathcal{F}_{\uparrow\downarrow}(\mathbf{k}, \tau) \equiv -\langle \mathcal{T}_\tau c_{-\mathbf{k}\downarrow}^\dagger(\tau) c_{\mathbf{k}\uparrow}^\dagger \rangle$. The calculation can be generalised to the $j \neq j'$ case by introducing a phase displacement operator D_φ .

Definition 1. *The unitary phase displacement operator*

for the subsystem A is defined by

$$D_{\varphi_A} \equiv \exp\left(i\frac{\varphi_A}{2} \sum_{\mathbf{k}} c_{\mathbf{k}\uparrow}^\dagger c_{\mathbf{k}\uparrow} + c_{-\mathbf{k}\downarrow}^\dagger c_{-\mathbf{k}\downarrow}\right), \quad (52a)$$

$$= \exp\left(i\frac{\varphi_A}{2} \hat{N}\right), \quad (52b)$$

and thus the phase displacement operator of the ajointed system $\mathcal{H}_A \otimes \mathcal{H}_B$ is given by $D_{\varphi_{AB}} = D_{\varphi_A} D_{\varphi_B}$. The action of the shift operator is to shift the phase of the BCS state:

$$D_\varphi |\Psi(\phi)\rangle = |\Psi(\phi + \varphi)\rangle. \quad (53)$$

With D_φ , the matrix element of the second-order term of the projection, is given by

$$\begin{aligned} \langle \Psi(\phi_j) | H_T(E_0\bar{P} - \bar{P}H_0\bar{P})^{-1}H_T | \Psi(\phi_{j'}) \rangle \\ = \langle \Psi(\phi_j) | H_T(E_0\bar{P} - \bar{P}H_0\bar{P})^{-1}H_T D_\varphi | \Psi(\phi_{j'}) \rangle, \\ = \langle H_T(\tau) H_T D_\varphi \rangle, \end{aligned} \quad (54a)$$

$$\begin{aligned} = 2 \sum_{\mathbf{k}_A \mathbf{k}_B} t^2 e^{i\phi_j} \mathcal{F}_{\uparrow\downarrow}(\mathbf{k}_A, \tau) \mathcal{F}_{\downarrow\uparrow}(\mathbf{k}_B, -\tau) \\ \times \langle \Psi(\phi_j) | \Psi(\phi_{j'}) \rangle + \text{c.c.} \end{aligned} \quad (54b)$$

After some algebra, we obtain

$$\begin{aligned} \langle \Psi(\phi_j) | H_T (E_0 \bar{P} - \bar{P} H_0 \bar{P})^{-1} H_T | \Psi(\phi_{j'}) \rangle & \quad (55) \\ = 2t^2 e^{i\phi_j} \frac{2N_A^e N_B^e}{b^2 - 1} \mathcal{I}(E_0, \Delta), \end{aligned}$$

where

$$\mathcal{I}(E_0, \Delta) = \begin{cases} \frac{\pi^2}{2\Delta} \left(1 - \frac{E_0^2}{16\Delta^2} \right), & \text{for } E_0 \ll \Delta \\ \frac{\pi \ln(2E_0/\Delta)}{2E_0}, & \text{for } E_0 \gg \Delta \end{cases}. \quad (56)$$

Details of the derivations of eq. (54) and eq. (56) are given in appendix C. In eq. (56), E_0 symbolises the energy of the unperturbed Hamiltonian H_0 such that $E_0 = E_A + E_B + \lambda_C N_A^e N_B^e$. By setting the zero-energy baseline as $E_A + E_B$, the unperturbed energy is roughly the Coulomb interaction between the two superconductors, which relates to the capacitance energy of the circuit: $E_0 \sim \lambda_C = E_C$. This capacitance energy is given by $E_C = (2e)^2/(2C)$, where the capacitance C is usually ~ 10 fF (or ~ 2 GHz) for Cooper-pair-box system, i.e., $E_C \sim 10^{-5}$ eV [22]. In general, the superconductor gap is $\sim 10^{-3}$ eV, such that $E_0/\Delta \sim 10^{-2}$, so we obtain $\mathcal{I} \approx \pi^2/2\Delta$.

Hence the second-order term of the projection is

$$\begin{aligned} & PH_T (E_0 \bar{P} - \bar{P} H_0 \bar{P})^{-1} H_T P \\ &= \sum_{j,j'} 2e^{i\phi_j} t^2 \frac{2N_A^e N_B^e}{b^2 - 1} \underbrace{\frac{\pi^2}{2\Delta} \langle \Psi(\phi_j) | \Psi(\phi_{j'}) \rangle | \Psi(\phi_j) \rangle \langle \Psi(\phi_{j'}) |}_{\approx \delta_{jj'}} \\ & \quad + \text{c.c.}, \\ & \approx \frac{t^2}{\Delta} \frac{4\pi^2 N_A^e N_B^e}{b^2 - 1} \cos \hat{\phi}, \end{aligned} \quad (57)$$

where we have defined $\cos \hat{\phi} = \sum_j \cos \phi_j | \Psi(\phi_j) \rangle \langle \Psi(\phi_j) |$. This is the expected functional form describing the effective Hamiltonian for the well-known Josephson junction. We comment on the details of this expression in section IV A 2.

D. Inductance: Spatial BCS Theory and Electromagnetic Fields

We have discussed the Coulomb interaction between metals and the electron tunneling inside the superconducting junction, which corresponds to the capacitance and the junction energy of the circuit, respectively. Here we are going to analyse the inductance part of the device. By applying a field to the system, the charge carriers will be accelerated, from which the kinetic inductance arises, and the electromagnetic energy will be transferred to the geometric inductance energy of the device. The complete manifestation is analysed in appendix E.

Here we consider a superconducting wire with finite cross-section area shown in fig. 7(a). For simplicity, we

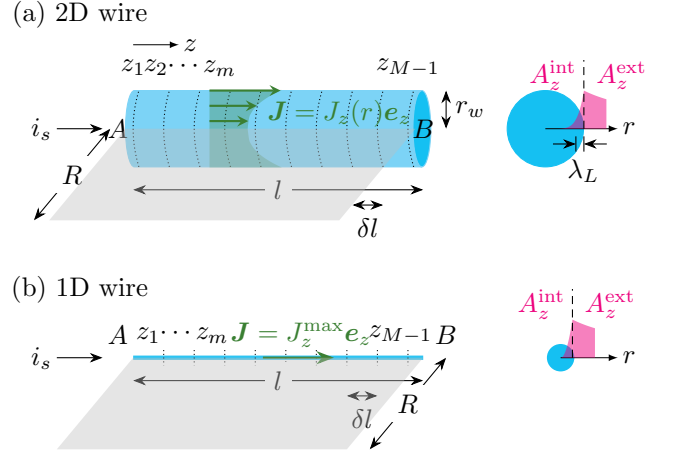


FIG. 7. (a) A cylindrically symmetric superconducting wire. The wire carries a supercurrent $i_s = \int_{\sigma} \mathbf{J} \cdot d\sigma$, which induces an internal field inside the superconductor (appendix E). The external magnetic field penetrates a small depth $\lambda_L = \sqrt{m/(\mu_0 D e^2)}$ into the superconductor, where D is the electron density in the material and m is electron mass. (b) The 1D approximation model to (a). We consider the effective cross-section area $\sigma_{\text{eff}} = \pi r_w^2 - \pi(r_w - \lambda_L)^2 \approx 2\pi r_w \lambda_L$, i.e., the area that the applied vector potential can penetrate into. The supercurrent in the 1D model is the maximal value in the 2D model: $\mathbf{J} = J_z^{\text{max}} \mathbf{e}_z$.

will take the wire to be cylindrical, so that the problem is a 2D system (while realistic microelectronic wires are 3D). In the 2D case, the superconducting phase and the vector potential depend on both the axial and radial coordinates, z and r . However we seek to describe the problem as a quasi-1D wire, shown in fig. 7(b), characterised by an axially varying phase, $\phi(z)$.

Our goal is to derive the constitutive relation and the relevant Hilbert space for a lumped inductive element from the microscopic wavefunction of a distributed, spatially-varying phase in superconducting wire of length l .

Classically, the current density, $\mathbf{J}(\mathbf{r})$, in a superconductor is related to the vector potential, $\mathbf{A}^{\text{int}}(\mathbf{r})$, by [23]

$$\mathbf{J}(\mathbf{r}) = \frac{1}{\mu_0} \nabla \times \nabla \times \mathbf{A}^{\text{int}}(\mathbf{r}), \quad (58)$$

where $\mathbf{A}^{\text{int}}(\mathbf{r})$ is the vector potential on the interior of the wire, and $\mathbf{J}(\mathbf{r}) = J_z(r) \mathbf{e}_z$ is axially symmetric. For convenience we choose a gauge in which the vector potential is also axially symmetric, so that

$$\mathbf{A}(\mathbf{r}) = A_z(r) \mathbf{e}_z. \quad (59)$$

In this axially symmetric gauge, we solve eq. (58) to find

$$A_z^{\text{int}}(r) = -\mu_0 \int_0^r dr' r' \log(r/r') J_z(r'). \quad (60)$$

More generally, we see that the gauge field inside the

superconductor is a linear functional of the current density,

$$\mathbf{A}^{\text{int}} = \mathbf{A}^{\text{int}}[\mathbf{J}], \quad (61)$$

which we use in subsequent analysis, below. The total current in the wire is the integral of the current density over a cross-section $\sigma = \pi r_w^2 e_z$, i.e. $i_s \equiv \int_{\sigma} \mathbf{J} \cdot d\sigma$. Since the system is linear, the current density will scale linearly with total current in the wire $\mathbf{J}(\mathbf{r}) = i_s \mathbf{j}(\mathbf{r})$, where \mathbf{j} is the normalised current density profile satisfying $\int_{\sigma} \mathbf{j} \cdot d\sigma = 1$, which carries information about the specific geometry of the wire. Putting these functional forms together, we have the general result

$$\mathbf{A}^{\text{int}} = i_s \mathbf{A}^{\text{int}}[\mathbf{j}], \quad (62)$$

indicating that the vector potential inside the superconductor scales linearly in the total current carried by the wire.

We assume that the 2D model can be approximated by a 1D wire shown in fig. 7(b), which is characterised by an axially-varying phase, $\phi(z)$, by analogy with the classical description above. Formally, we discretise the wire into $M \gg 1$ segments, so that the discretised Hilbert space of the wire is $\mathcal{H}_{\text{wire}} = \mathcal{H}_A \otimes \mathcal{H}_{z_1} \otimes \cdots \otimes \mathcal{H}_B$, in a basis spanned by states of the form

$$\begin{aligned} |\Psi(\phi(z))\rangle &= |\Psi_A(\phi_A)\rangle \otimes |\Psi_{z_1}(\phi_{z_1})\rangle \otimes \cdots \otimes |\Psi_B(\phi_B)\rangle, \\ &\equiv \bigotimes_z |\Psi_z(\phi(z))\rangle, \end{aligned} \quad (63)$$

where z labels both the tensor-product element along the discretised wire, and the phase coordinate at each position. In this formulation, there is a local compact Hilbert space associated to each segment

Compared to the point-like Josephson junction and capacitor model, the (distributed) inductive element has a significantly larger Hilbert space, which will become important below. As before we use this basis to define the low energy projector

$$\begin{aligned} \Pi &= \sum_{\phi(z)} \bigotimes_z |\Psi_z(\phi(z))\rangle \langle \Psi_z(\phi(z))|, \\ &= \bigotimes_z \sum_{\phi(z)} |\Psi_z(\phi(z))\rangle \langle \Psi_z(\phi(z))|, \\ &= \bigotimes_z P_z, \end{aligned} \quad (64)$$

where $P_z = \sum_{\phi(z)} |\Psi_z(\phi(z))\rangle \langle \Psi_z(\phi(z))|$ defines a projector, like eq. (12), at each of the discretised locations, z , along the wire. Similarly, we define a phase-field, and gradient operators

$$\hat{\phi}(z) = \bigotimes_z \sum_{\phi(z)} \phi(z) |\Psi_z(\phi(z))\rangle \langle \Psi_z(\phi(z))|, \quad (65)$$

$$\hat{\phi}'(z) = \bigotimes_z \sum_{\phi(z)} \phi'(z) |\Psi_z(\phi(z))\rangle \langle \Psi_z(\phi(z))|. \quad (66)$$

1. Inductive constitutive law

Using the second quantised form of the field operators $\psi_{\mathbf{r}} = e^{i\phi(z)/2} c_{\mathbf{r}}$ (where we suppress the spin label s), the (quantised) supercurrent density operator is given by [24, 25]

$$\hat{\mathbf{J}}(\mathbf{r}) = \frac{e}{2m} \left(\psi_{\mathbf{r}}^\dagger (\hat{\mathbf{p}} - 2e\hat{\mathbf{A}}^{\text{int}}) \psi_{\mathbf{r}} + \text{h.c.} \right), \quad (67)$$

where $\hat{\mathbf{A}}^{\text{int}}(r) = \mathbf{A}^{\text{int}}[\hat{\mathbf{J}}]$ is a linear functional of the current density operator, from eq. (59). In the effective low energy subspace, the supercurrent density operator is given by the projection onto the low energy subspace

$$\begin{aligned} \hat{\mathbf{J}}^{\text{eff}}(r, z) &= \Pi \hat{\mathbf{J}} \Pi \\ &= \bigotimes_z \sum_{\phi(z), \bar{\phi}(z)} \langle \Psi_z(\phi(z)) | \hat{\mathbf{J}}(\mathbf{r}) | \Psi_z(\bar{\phi}(z)) \rangle \\ &\quad \times |\Psi_z(\phi(z))\rangle \langle \Psi_z(\bar{\phi}(z))|, \\ &\approx \bigotimes_z \sum_{\phi(z)} \langle \Psi_z(\phi(z)) | \hat{\mathbf{J}}(0) | \Psi_z(\phi(z)) \rangle \\ &\quad \times |\Psi_z(\phi(z))\rangle \langle \Psi_z(\phi(z))|, \\ &= \bigotimes_z \sum_{\phi(z)} \mathbf{J}(r, z) |\Psi_z(\phi(z))\rangle \langle \Psi_z(\phi(z))|, \end{aligned} \quad (68)$$

where we have used the (approximate) orthonormality of the set $\{|\Psi(\phi(z))\rangle\}$ for each z (see eq. (21)), and

$$\begin{aligned} \mathbf{J}(r, z) &= \langle \Psi(\phi) | \hat{\mathbf{J}}(r, z) | \Psi(\phi) \rangle, \\ &= \frac{De^2}{m} \left(\frac{\Phi_0}{2\pi} \phi'(z) \mathbf{e}_z + \mathbf{A}^{\text{int}}(r) \right), \end{aligned} \quad (69)$$

where m is the electron mass, e is the electron charge, and D is the electron density. eq. (69) agrees with the mean-field theory current density in a wire arising from the gauge invariant phase [24]. Putting together eq. (68) and eq. (69), we find the current density operator in the low-energy BCS subspace is given by

$$\hat{\mathbf{J}}^{\text{eff}}(r, z) = \frac{De^2}{m} \left(\frac{\Phi_0}{2\pi} \hat{\phi}'(z) \mathbf{e}_z + \mathbf{A}^{\text{int}}[\hat{\mathbf{J}}^{\text{eff}}] \right). \quad (70)$$

We are concerned with the mesoscopic properties of the wire, integrated over the cross section. The total integrated current operator is

$$\begin{aligned} \hat{i}_s &= 2\pi \int_0^{r_w} dr r \hat{J}_z(r), \\ &= \frac{De^2}{2m} \left(\Phi_0 \hat{\phi}'(z) r_w^2 - \hat{i}_s \mu_0 \lambda_L \left(2\lambda_L - \frac{r_w}{I_1(r_w/\lambda_L)} \right) \right), \end{aligned} \quad (71)$$

where the second line is computed for a cylindrically symmetric geometry. In the limit $\lambda_L \ll r_w$, $I_1(r_w/\lambda_L)^{-1}$ is exponentially suppressed, and we solve eq. (71) for the current operator $\hat{i}_s(z)$ within each wire segment

$$\hat{i}_s(z) \approx \frac{\Phi_0}{2\pi} \hat{\phi}'(z) \frac{l}{\frac{m}{De^2} \frac{l}{\pi r_w^2} + \frac{\mu_0 l}{8\pi}} = \frac{\Phi_0}{2\pi} \hat{\phi}'(z) / \bar{L}, \quad (72)$$

where the total inductance per unit length is given by $\bar{L} = (L_K + L_G)/l$, which consists of the geometric inductance of a wire of length l , $L_G = \mu_0 l/(8\pi)$ (which agrees with the usual calculation of L_G up to a logarithmic factor in eq. (E15)), and the kinetic inductance $L_K = \frac{m}{De^2} \frac{l}{\sigma}$, where $\sigma = \pi r_w^2$ is the cross-sectional area of the wire.

Finally, we make the ‘‘lumped element approximation’’, in which $\hat{\phi}'(z)$ is assumed to be determined by the boundary values $\hat{\phi}_{A,B} \equiv \hat{\phi}(z_{A,B})$, i.e., the phase-field operator simply interpolates between the phase operator $\hat{\phi}'(z) = (\hat{\phi}_B - \hat{\phi}_A)/l$, so that there is only a single current operator associated to the wire, given by

$$\hat{i}_s = (\hat{\Phi}_B - \hat{\Phi}_A)/L, \quad (73)$$

where $L = \bar{L}l$ and $\hat{\Phi}_{A,B} = \frac{\Phi_0}{2\pi} \hat{\phi}_{A,B}$ is the usual mesoscopic integrated nodal flux coordinate associated to the end points of the wire. This agrees with the usual constitutive inductive relation between current and flux.

2. Effective Hamiltonian of an inductor

Here we consider the spatial dependence of the fermionic Hamiltonian eq. (1) and derive the effective inductor Hamiltonian in \mathcal{H}_{BCS} with the projector Π . In the position basis in the presence of a vector potential, the electronic kinetic term in the island Hamiltonian H_A from eq. (2) is given by

$$H_{K_A} = \int_{\text{SC}} dV c_{rs}^\dagger \left[\frac{1}{2m} (\mathbf{p} + q\mathbf{A}^{\text{int}})^2 - \mu \right] c_{rs}. \quad (74)$$

The effective inductance Hamiltonian is given by the projection $\Pi(H_{K_A} + H_{I_A})\Pi$, in which the interaction contributes a constant term $\mathcal{V}(\varphi)$, as in eq. (39). Below we consider only the projection of the electronic kinetic Hamiltonian. For simplicity, we remove the z -dependence by introducing the gauge transformation $\mathcal{G}_{\phi(z)} = e^{i\phi(z)\hat{N}/2}$ and compute the projection $\Pi H_{K_A}\Pi$ (detail can be referred from eq. (D5) to eq. (D10)):

$$\begin{aligned} \Pi H_{K_A}\Pi &= \bigotimes_z \sum_{\phi(z), \bar{\phi}(z)} \langle \Psi_z(\phi(z)) | H_{K_A} | \Psi_z(\bar{\phi}(z)) \rangle \\ &\quad \times | \Psi_z(\phi(z)) \rangle \langle \Psi_z(\bar{\phi}(z)) |, \\ &\approx \bigotimes_z \sum_{\phi(z)} \langle \Psi_z(\phi(z)) | H_{K_A} | \Psi_z(\phi(z)) \rangle \\ &\quad \times | \Psi_z(\phi(z)) \rangle \langle \Psi_z(\phi(z)) |, \\ &= \frac{1}{2} \frac{De^2}{m} \int_{\text{SC}} dV \left(\frac{\Phi_0}{2\pi} \hat{\phi}'(z) - A_z^{\text{int}}(\hat{i}_s) \right)^2, \end{aligned}$$

where A_z^{int} is the vector potential inside the superconducting wire that couples to the current operator eq. (72). Considering the superconducting wire with cylindrical symmetry and adopting $A_z^{\text{int}}(\hat{i}_s) = \hat{i}_s \frac{\mu_0 \lambda_L}{2\pi r_w} \frac{1 - I_0(r/\lambda_L)}{I_1(r_w/\lambda_L)}$

from eq. (E6) and expressing \hat{i}_s in terms of $\hat{\phi}'$ by eq. (72), we obtain

$$\Pi H_{K_A}\Pi \approx \frac{1}{2} \left(\frac{\Phi_0}{2\pi} \right)^2 \frac{1}{\bar{L}} \int_0^l dz \hat{\phi}'^2(z), \quad \text{for } \lambda_L \ll r_w. \quad (75)$$

Details of the integration are given in eq. (D12).

3. Lumped Element Inductive Energy

To evaluate the integral of $\hat{\phi}'(z)$ in eq. (75), we consider the lumped element approximation, $\hat{\phi}' = (\hat{\phi}_B - \hat{\phi}_A)/l$, so that $\int_0^l dz \hat{\phi}'^2 = \hat{\phi}_{AB}^2/l \equiv \hat{\phi}^2/l$. eq. (75) now becomes

$$\Pi H_{K_A}\Pi = \frac{1}{2L} \left(\frac{\Phi_0}{2\pi} \right)^2 \hat{\phi}^2 = \frac{E_L}{2} \hat{\phi} \equiv H_L, \quad (76)$$

where the inductance energy is defined by $E_L \equiv (\frac{\Phi_0}{2\pi})^2/L$. Note that here we choose the energy baseline to be $\mathcal{V}(\varphi) = \Pi H_{I_A}\Pi = 0$, where $\varphi = \hat{\phi} - \phi$. The phase operator $\hat{\phi}$ denotes the phase difference across the superconductor.

On the other hand, let’s evaluate the Hamiltonian of the entire wire from the summation over all segments. Each element is described by the Hamiltonian

$$H_{\text{seg}} = \frac{1}{2L \cdot \delta l} \left(\frac{\Phi_0}{2\pi} \right)^2 (\delta \hat{\phi})^2 = \frac{E_L}{2} M (\delta \hat{\phi})^2, \quad (77)$$

where $\delta l = l/M$ is the unit length. For the m -th segment, the phase drop is $\delta \hat{\phi}_m = \hat{\phi}_{m+1} - \hat{\phi}_m$ and $H_{\text{seg}} = H_{\text{seg}}(m)$. The Hamiltonian of the wire is then given by the sum,

$$H_{\text{wire}} = \sum_{m=z_A}^{z_B} H_{\text{seg}}(m) = \frac{E_L}{2} M \sum_{m=z_A}^{z_B} (\hat{\phi}_{m+1} - \hat{\phi}_m)^2, \quad (78)$$

and $H_{\text{wire}} \in \mathcal{H}_A \otimes \dots \otimes \mathcal{H}_B$. Given the boundary values of the phase $\hat{\phi}_A, \hat{\phi}_B$, we minimise H_{wire} with respect to $\{\phi_{z_2}, \dots, \phi_{z_{M-1}}\}$, having

$$\begin{aligned} \hat{\phi}_{z_2} - \hat{\phi}_{z_A} &= \hat{\phi}_{z_3} - \hat{\phi}_{z_2}, \\ \hat{\phi}_{z_3} - \hat{\phi}_{z_2} &= \hat{\phi}_{z_4} - \hat{\phi}_{z_3}, \\ &\vdots \\ \hat{\phi}_{z_{M-1}} - \hat{\phi}_{z_{M-2}} &= \hat{\phi}_{z_B} - \hat{\phi}_{z_{M-1}}, \end{aligned}$$

such that $\delta \hat{\phi}$ is constant and $\hat{\phi}_B - \hat{\phi}_A = M \cdot \delta \phi$, which agree with the lumped element assumption. Hence we rewrite the sum $\sum_m (\hat{\phi}_{m+1} - \hat{\phi}_m)^2 \approx (\hat{\phi}_B - \hat{\phi}_A)^2/M$ and obtain

$$H_{\text{wire}}^{\text{min}} = \frac{E_L}{2} (\hat{\phi}_B - \hat{\phi}_A)^2 = \frac{E_L}{2} \hat{\phi}^2. \quad (79)$$

Now the Hilbert space reduces to $H_{\text{wire}}^{\text{min}} \in \mathcal{H}_A \otimes \mathcal{H}_B$ while the phase $\hat{\phi} \equiv \hat{\phi}_B - \hat{\phi}_A \in [-\pi, \pi)$ depends only on the boundary values.

4. Emergent Low-energy Hilbert Space of an Inductor

While we have described a point-like superconducting element (e.g. a capacitor or tunnel junction) with a periodic coordinate $\phi \in [-\pi, \pi]$, which respects the translation symmetries of these devices, the inductive constitutive law eq. (73) breaks translation symmetry, and the Hilbert space of ϕ_{AB} is substantially larger. Here we provide an physically-motivated argument that bounds the physically relevant Hilbert space for an inductive element.

As discussed above, the discretised 1D inductor is formed from M segments, and recalling the definition of $\mathcal{Z} \in [-\pi, \pi]$, the natural Hilbert space for the wire is

$$\mathcal{H}_{\text{wire}} = \mathcal{H}_A \otimes \cdots \otimes \mathcal{H}_B = \mathcal{Z}^{\otimes M-1}, \quad (80)$$

where the exponent $M-1$ indicates that the relevant internal degrees of freedom are the relative phases $\Delta\phi_j = \phi_{z_j+1} - \phi_{z_j} \in \mathcal{Z} \subset [-\pi, \pi]$ between neighbouring segments.

The subsequent ‘‘lumped-element’’ approximation treats dynamics of the interior segments as being determined by the boundary values $\phi_{A,B}$, and so the accessible states within $\mathcal{H}_{\text{wire}}$ satisfy $\Delta\phi_j = (\phi_B - \phi_A)/M$ for each j . It follows that $\phi_B - \phi_A \in M[-\pi, \pi]$, which determines the effective, lumped element Hilbert space of the discretised wire.

We next note that M is bounded by the physical constraint that the supercurrent must be below the critical current, i_c , of the wire. In particular, the total current in the wire is $|i_s| = \Phi_0|\phi_B - \phi_A|/L \leq \Phi_0 M \pi / L < i_c$, and so

$$M \leq M_{\text{max}} = i_c L / \Phi_0. \quad (81)$$

This maximal number depends on the gap and the temperature because $i_c = \frac{\Delta}{\lambda_L(T)} \sqrt{\frac{\rho_F}{2\mu_0}}$. Though the phase operator $\hat{\phi}$ is still compact it is no longer periodic, since lumped-element states with $\phi_{AB} = \pm\pi M$ correspond to opposite current flows.

We comment in passing that this argument really asserts that the dissipationless description of the inductive element requires the phase drop across the inductor to be bounded in the interval $\phi_{AB} \in M[-\pi, \pi]$. However, the discretisation imposed here is not physical, and so it is physically possible for ϕ_{AB} to exceed this range, at which point the current exceeds the critical value, and the system becomes dissipative via quasiparticle formation. A more formal treatment of this would require the inclusion of these states in a larger Hilbert space. This is beyond the goals of this work, and we leave this to future research.

E. Effective LCJ Hamiltonian

Eventually, an LCJ circuit in the presence of the external magnetic flux is described by the Hamiltonian

$$H_{\text{LCJ}} \approx 4E_C \hat{N}_A \hat{N}_B - E_J \cos \hat{\phi} + \frac{E_L}{2} \hat{\phi}^2. \quad (82)$$

By expressing the energy coefficients E_C , E_J and E_L in terms of the physical quantities in the superconductivity, we connect the microscopic theory to the conventional macroscopic picture of the LCJ circuit. eq. (82) is derived in the absence of the bias field; however, the additional field can be included and will enter the Hamiltonian as a phase shift [26, 27] in the inductance term. Different choice of energy ratio among the energy coefficients results in various (e.g. heavy, light, low/high impedance) potential landscapes of superconducting qubits [28].

IV. DISCUSSION

A. Effective Capacitor-Junction Hamiltonian

The combination of eq. (48), eq. (50), eq. (57) gives the effective Hamiltonian of the JC circuit in the ground subspace \mathcal{H}_0 :

$$H_{\text{JC}} = 4\lambda_C \hat{N}_A \hat{N}_B + \frac{t^2}{\Delta} \frac{4\pi^2 N_A^e N_B^e}{b^2 - 1} \cos \hat{\phi}. \quad (83)$$

Comparing to the conventional CPB model [29], we can express the capacitance and junction energies E_C , E_J in terms of the physical quantities of the superconducting device:

$$E_C = \lambda_C, \quad E_J = -\frac{t^2}{\Delta} \frac{4\pi^2 N_A^e N_B^e}{b^2 - 1}. \quad (84)$$

eq. (84) establishes the connection between the microscopic picture to the conventional macroscopic picture and allows us to obtain the relevant energies without experimental measurements. The effective Hamiltonian eq. (83) is derived from first principles without passing through any classical approach and hence is fully-quantum. As the phase operator $\hat{\phi}$ arises from the matter phase of the BCS state $|\Psi(\phi)\rangle$ such that $\phi \in [-\pi, \pi]$, it is a compact variable.

1. Energetics of a JC Circuit

Recalling the number-phase uncertain relation of a Josephson junction eq. (36), the additional term $-2\pi\delta(\phi_0 - \phi)$ arises from the compactness of the Hilbert space, in which the raising operator in number is given by [16]

$$\begin{aligned} e^{i\hat{\phi}} = & |0\rangle\langle 1| + |1\rangle\langle 2| + \cdots + |j_{\text{max}} - 1\rangle\langle j_{\text{max}}| \\ & + e^{i(j_{\text{max}}+1)\phi_0} |j_{\text{max}}\rangle\langle 0|. \end{aligned} \quad (85)$$

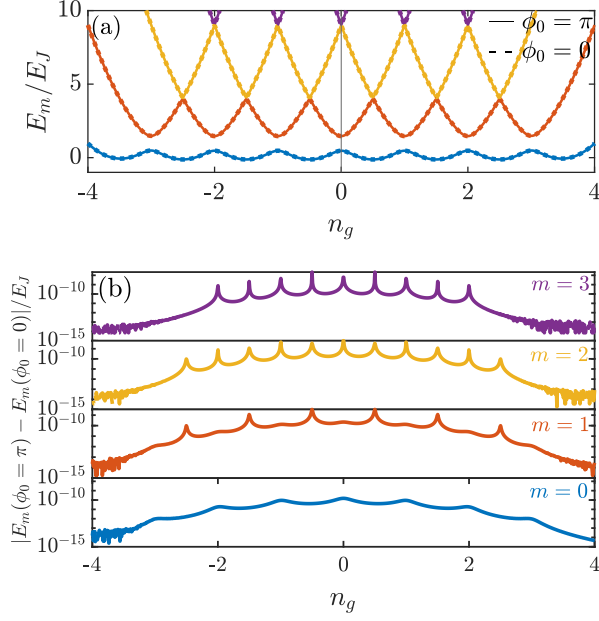


FIG. 8. (a) The eigenenergies E_m for the first four levels of a transmon eq. (86) for a $j_{\max} = 8$ -electron system with $E_J = E_C$. The solid thin lines are with the reference phase $\phi_0 = \pi$, while the dashed lines are with $\phi_0 = 0$. The maximal energy difference between each solid and dashed is of the order $\mathcal{O}(10^{-10})$ and thus can be viewed as overlap. All energies are scaled by E_J . (b) Energy differences between two choices of reference phase ($\phi_0 = \pi, 0$) for $m = 0, 1, 2, 3$ levels.

Here $j_{\max} = \sqrt{n-1}/\alpha$ is the maximal number state of the system. Rewrite H_{JC} as

$$H_{JC}(\phi_0) = 4E_C \left(\hat{N} - n_g \right)^2 - \frac{E_J}{2} \left(e^{i\hat{\phi}} + e^{-i\hat{\phi}} \right), \quad (86)$$

of whom we can compute the eigenenergies with respect to different reference phase ϕ_0 . By increasing the total number of the particles, j_{\max} , the energy difference with respect to the largest reference phase difference π of a given level becomes smaller. According to fig. 8, by setting the total number of electrons $j_{\max} = 8$, the maximal energy difference $|E_m(\phi_0 = \pi) - E_m(\phi_0 = 0)|$ is of the order $\mathcal{O}(10^{-10}E_C)$ for $E_C = E_J$, and is hence negligible. Thanks to the rare contribution of the reference phase ϕ_0 , the spectrum in compact and non-compact space are highly overlap. Consequently, the canonical relationship between \hat{N} and $e^{i\hat{\phi}}$ is approximately the same in compact and non-compact space in practical.

2. Comparison with Experiments

Here we estimate the junction and capacitance energies in eq. (84) and compare them with a measurement outcome. In the experiment [30], the Josephson junction is made by aluminium, which as gap $\Delta \approx 200$ μeV and electronic bandwidth $B \approx 1.68$ eV (i.e., $b \approx 8.4 \times$

10^3). The measured energies are $E_J^{\exp} = 210$ μeV and $E_C^{\exp} = 90$ μeV . The two aluminium islands are separated by an aluminium oxide as the insulating barrier. Every aluminium atom contributes an electron to the circuit since its electron configuration is $[\text{Ne}]3s^23p^1$, i.e., only a single electron on its most outer p -orbital. The number of electrons on each island, N^e , is then roughly the that of the aluminium atoms. Given the junction dimension parameters, we obtain $N_A^e \approx 1.02 \times 10^8$, $N_B^e \approx 1.43 \times 10^8$.

Microscopic tunneling from WKB method: We model the junction by the one-dimensional double-well potential in fig. 9 (a). At low temperature, the electrons travel with Fermi velocity v_F , colliding with the will with an “attempt” frequency $f_{A,B} = v_F/(2l_{A,B})$. A symmetric junction has $f_A \approx f_B \equiv f$. According to WKB method, the tunnel matrix element t is given by

$$t = hf \cdot T = hf \cdot e^{-2l_I \sqrt{2m_e^* U_0}/\hbar}, \quad (87)$$

where T is the tunneling probability, l_I is the thickness of the insulator, and m_e^* is the effective electron in the superconductor ($m_e^* = 0.4m_e$ for aluminium oxide). The potential height U_0 is measured by the Fermi level, and depends on the thickness l_I and the material [31]. The barrier’s height ranges between 2 eV \sim 2.5 eV for the thickness 2.5 nm \sim 70 nm [32, 33]. Given the Fermi velocity of aluminium $v_F \approx 2.03 \times 10^6$ m/s, the collision frequencies are $f_A \approx 41$ THz, $f_B \approx 29$ THz. We can then estimate E_J with eq. (84). However, the uncertainty of the parameters in tunnel matrix element results in huge error exponentially. We describe the error in T by the correction formula

$$T_\beta = e^{-2l_I \sqrt{2\beta m_e^* U_0}/\hbar}, \quad (88)$$

where β denotes the possible error from the insulator thickness l_I , potential height U_0 , and the effective mass m_e^* . fig. 9 (b) shows that a small vary in β leads to a exponential change in E_J . Our estimation has an error $\beta \approx 2$ comparing to the measured E_J in the experiment [30].

Coulomb energy: The capacitance energy relates to the Coulomb interactions. Suppose each superconductor has the net charge $Q_j^n - Q_j^e$, $j = A, B$, where Q_j^n is the charge of nucleus. The electric potential energy is given by

$$E_{\text{Coul}} = \frac{-1}{4\pi\epsilon} \frac{(Q_A^n - Q_A^e)(Q_B^n - Q_B^e)}{l_I + \frac{1}{2}(l_A + l_B)}, \quad (89)$$

where ϵ is the permittivity of the superconductor at working temperature of the device. According to the electric neutrality, we have the condition

$$Q_A^n + Q_B^n = Q_A^e + Q_B^e. \quad (90)$$

eq. (89) becomes

$$E_{\text{Coul}} = \frac{e^2}{4\pi\epsilon} \frac{(N_A^n - N_A^e)^2}{l_I + \frac{1}{2}(l_A + l_B)} \equiv \lambda_C. \quad (91)$$

The electric potential energy is clearly in the form of the capacitance energy: $E_{\text{Coul}} \propto Q^2$.

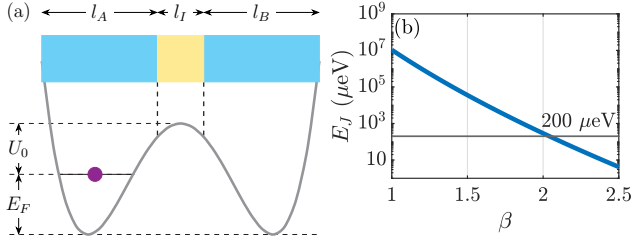


FIG. 9. (a) We estimate the tunnel matrix element t by WKB approach in a double-well potential approximation. The oxide layer acts as the barrier, whose energy is U_0 -higher than the electron energy inside the superconductors. Assume the electrons inside the superconductor is moving with speed v_F , which corresponds to the Fermi energy E_F . (b) The estimated junction energy with different error parameter β in tunneling rate. Here we consider the symmetric junction, $l_A \approx l_B$ such that $f_A \approx f_B$, and approximate t as a constant: $t \equiv t_A = t_B$.

3. WKB in Non-Zero Magnetic Fields

Consider a Josephson junction in an additional field described by \mathbf{A} . The tunnel matrix element is oscillatory in phase [34]

$$t' = t e^{i \int_{\mathbf{l}} \mathbf{A} \cdot d\mathbf{l} / \Phi_0} = t e^{i \Phi_b l_I / ((l_A + l_B + l_I) \Phi_0)}, \quad (92)$$

where t is the regular tunnel matrix element without fields, \mathbf{l} is the tunneling path, and Φ_b is the bias magnetic flux threading the device. The tunneling Hamiltonian gains a phase shift in t , becoming

$$E_J \cos \hat{\phi} \mapsto E_J \cos \left(\hat{\phi} - \frac{l_I}{l_A + l_B + l_I} \frac{\Phi_b}{\Phi_0} \right), \quad (93a)$$

$$\approx E_J \cos \hat{\phi}, \quad \because l_I \ll l_A + l_B. \quad (93b)$$

The phase shift is negligible as the insulator layer of a junction is usually thin comparing to the electrodes. As the bias field Φ_b has significant contribution in the inductance term as a phase shift $2\pi\phi_b/\Phi_0$ [27], we see the ambiguity in compactness of the superconducting phase $\hat{\phi}$.

B. Higgs Modes

Consider the ground-state energy of a superconducting island eq. (41) in the absence of the fields here. We rescale E_A and Δ_A by E_A^{\min} and Δ_A^{\min} . Define $d \equiv \Delta_A / \Delta_A^{\min}$, so

$$\mathcal{E} \equiv \frac{E_A}{E_A^{\min}}, \quad (94)$$

$$= d^2 (-1 + 2 \ln d - 2\lambda(\ln d)^2) + \mathcal{O}\left(\frac{1}{b^3}\right), \quad (94)$$

$$\approx 2(1 - \lambda)(d - 1)^2 - 1 + \mathcal{O}(d^3). \quad (95)$$

fig. 10 shows \mathcal{E} calculation from eq. (94) and from the quadratic approximation in eq. (95). Varying ϕ , \mathcal{E} is the well-known ‘Mexican-hat’ potential, with the quadratic approximation applied near the minimum. Note that \mathcal{E} is not analytic at $\Delta = 0$. Quantum mechanically there will preserve excitations of the Higgs mode, and the superconducting devices will more generally be defined over a Hilbert space $\{|\Psi(\phi, \Delta)\rangle\}$, where ϕ is the azimuthal angle of the Mexican hat and Δ is the radial coordinates shown in fig. 10 (b). While the phase mode (or Nambu-Goldstone mode) is massless according to the symmetry, the (gap) amplitude mode (or Higgs mode) is massive due to the energy costs for excitations.

The Higgs mode of superconductors can be excited resonantly by a driven field with energy at Δ , and oscillates at frequency $\omega_{\text{Higgs}} = 2\Delta^{\min}/\hbar$ [10]. By treating the Higgs mode excitations as a harmonic oscillator with the quadratic potential eq. (95), we obtain the effective mass of the oscillator associated with the potential $E_A(\mathcal{B}, \Delta)$:

$$m^* \approx \frac{\hbar^2(1 - \lambda)}{4} \cdot \frac{1}{\rho^2(E_F) E_A^{\min}}. \quad (96)$$

The depth of the Higgs potential in fig. 10 can be expressed in terms of ω_{Higgs} , and we have the number of excitations:

$$\# \text{ excitations} = \frac{|E_A^{\min}|}{\hbar \omega_{\text{Higgs}}} = \frac{n e^{-1/\lambda}}{4}. \quad (97)$$

Now the BCS ground state can be expressed as a function of gap $|\Psi(\phi, \Delta)\rangle$. The overlap is then given by

$$\mathcal{Y}(\Delta, \Delta') = \langle \Psi(\phi, \Delta) | \Psi(\phi, \Delta') \rangle \approx e^{-\frac{3n\pi(\Delta' - \Delta)^2}{128\sqrt{2b}\Delta^2}}, \quad (98)$$

which is evaluated by the similar procedures for $\mathcal{W}(\phi)$. The overlap eq. (98) is approximately a Gaussian with width $\sim \sqrt{(\mathcal{B}\Delta)/n}$. Namely, the maximal number of Higgs modes in the potential well $E_A(\mathcal{B}, \Delta)$ for a given phase ϕ is roughly $\sim \sqrt{n e^{-1/\lambda}}$.

V. CONCLUSION

We propose a fully-quantum approach to the quantisation of superconducting circuits in this paper. By restricting to the low-energy sector, we derive the effective Hamiltonian of the superconducting LCJ circuit from first principles. With the fully-quantum framework, we establish the connection between the microscopic and the macroscopic pictures. Taking a standard LCJ circuit for instance, (1) the Coulomb interaction between the two superconductors gives rise to the capacitance part; (2) each electron tunneling contributes an additional phase to the junction energy; (3) the electromagnetic field inside and outside the device relate to the inductance energies. From the energy point of view, the magnetic flux

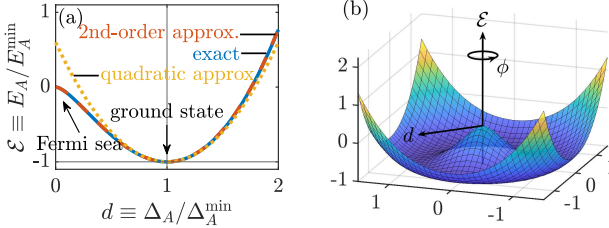


FIG. 10. (a) The scaled energy spectrum E_A/E_A^{\min} with respect to the scaled order parameter $d \equiv \Delta_A/\Delta_A^{\min}$. The second-order approximation eq. (41a) (orange dashed) perfectly fits the exact solution (blue solid) in the physical region. At Δ_A^{\min} , we obtain the minimum of the energy spectrum which corresponds to the gap parameter at zero temperature. We use the quadratic expansion eq. (95) (dotted yellow) to estimate the effective mass of the quasiparticle from the harmonic oscillator model. (b) The Mexican-hat potential well of the superconductor with respect to all possible ϕ in its ground-state subspace \mathcal{H}_0 . The spectrum is illustrated in cylindrical coordinates, in which we use the ratio d as the radial distance, the matter phase ϕ as the azimuth, and energy ratio \mathcal{E} as the height.

enters the circuit Hamiltonian as a phase shift, and contributes significantly only to the inductance term. During the derivation, we choose a discrete basis set for projection, and show that the required subspace dimension $\mathcal{O}(\sqrt{n})$ is much smaller than the total electron mode number n of the system. Moreover, we show that the subspace emerges, which is bounded by the critical current of the superconductor, as inductors are included to the circuit.

An analytical form to the Higgs modes in superconductors is provided in this paper. With quartic and quadratic approximations to the energy spectrum, we obtain the order parameter at zero-temperature and the effective mass of the oscillator, respectively.

Another highlight of the work is the ambiguity in compactness. Following the definition of the discrete basis set in phase domain, the matter phase ϕ has to be with a certain range, and therefore is compact. However, the inclusion of the external fields turns it into non-compact as the field is arbitrary. Nevertheless the discreteness and the non-compactness in phase have little affect to the canonical relation and the energy spectrum in practical.

Our approach is easily generalised to multilevel systems and the time-dependence can be included in the external field as well. While the constant field has no

effect to the capacitance energy, a time-varying field will enter in its time-derivative form. As the supercurrent determines the range of the phase operator, it breaks the BCS symmetry and therefore an open system has to be considered. By including the higher energy levels, who act as the dissipation channels, one can explore the contribution of the quasiparticles. In addition to the Josephson junction, more superconducting devices such as quantum phase slip (QPS) [35] can be explored by this approach, by simply substituting the device's Hamiltonian and compute the projection.

Appendix A: Eigenstate of Electron Number Operator

In this appendix, we show that the number state defined in eq. (25) is the eigenstate of both electron and Cooper pair number operators, \hat{N}^e , \hat{N} respectively.

Proof. The BCS state in N -representation is described by

$$|\Psi(N)\rangle = \left(\frac{\alpha}{\sqrt{n-1} + \alpha} \right)^{1/2} \times \sum_{j=0}^{\sqrt{n-1}/\alpha} e^{-iN\phi_j} \prod_{\mathbf{k}=\mathbf{k}_1}^{\mathbf{k}_n} (u_{\mathbf{k}} + v_{\mathbf{k}} e^{i\phi_j} c_{\mathbf{k}\uparrow}^\dagger c_{-\mathbf{k}\downarrow}^\dagger) |0\rangle. \quad (\text{A1})$$

We can expand the product of binomials in eq. (A1) into a sum of product by the lemma [36]:

Lemma 1. $\forall A_k, B_k$ such that $[A_k, B_k] = 0$, we have an identity

$$\prod_{k=1}^n (A_k + B_k) = \sum_{m=0}^n \sum_{\chi \in \mathcal{S}_m} \prod_{i \in \chi} A_i \prod_{j \in \chi^c} B_j,$$

where \mathcal{S}_m is the set of all subsets of $\{1, 2, \dots, n\}$ with exactly m elements, i.e.,

$$\mathcal{S}_m \equiv \{\chi \subseteq \{1, 2, \dots, n\}, |\chi| = m, \}, \quad |\mathcal{S}_m| = \binom{n}{m},$$

and χ^c is the complement of χ .

With a substitution $u_{\mathbf{k}} \rightarrow A_k$, $v_{\mathbf{k}} e^{i\phi_j} c_{\mathbf{k}\uparrow}^\dagger c_{-\mathbf{k}\downarrow}^\dagger \rightarrow B_k$, eq. (A1) becomes

$$|\Psi(N)\rangle = \left(\frac{\alpha}{\sqrt{n-1} + \alpha} \right)^{1/2} \sum_{j=0}^{\sqrt{n-1}/\alpha} e^{-iN\phi_j} \sum_{m=0}^n \sum_{\chi \in \mathcal{S}_m} \prod_{\mathbf{k}_i \in \chi^c} u_{\mathbf{k}_i} \prod_{\mathbf{k}_j \in \chi} v_{\mathbf{k}_j} e^{i\phi_j} c_{\mathbf{k}_j \uparrow}^\dagger c_{-\mathbf{k}_j \downarrow}^\dagger |0\rangle, \quad (\text{A2a})$$

$$\begin{aligned} &= \left(\frac{\alpha}{\sqrt{n-1} + \alpha} \right)^{-1/2} \frac{\alpha}{\sqrt{n-1} + \alpha} \sum_{j=0}^{\sqrt{n-1}/\alpha} e^{-iN\phi_j} \sum_{m=0}^n e^{im\phi_j} \sum_{\chi \in \mathcal{S}_m} \prod_{\mathbf{k}_i \in \chi^c} u_{\mathbf{k}_i} \prod_{\mathbf{k}_j \in \chi} v_{\mathbf{k}_j} c_{\mathbf{k}_j \uparrow}^\dagger c_{-\mathbf{k}_j \downarrow}^\dagger |0\rangle, \\ &= \left(\frac{\alpha}{\sqrt{n-1} + \alpha} \right)^{-1/2} \sum_{m=0}^n \left(\frac{\alpha}{\sqrt{n-1} + \alpha} \sum_{j=0}^{\sqrt{n-1}/\alpha} e^{i(m-N)\phi_j} \right) \sum_{\chi \in \mathcal{S}_m} \prod_{\mathbf{k}_i \in \chi^c} u_{\mathbf{k}_i} \prod_{\mathbf{k}_j \in \chi} v_{\mathbf{k}_j} c_{\mathbf{k}_j \uparrow}^\dagger c_{-\mathbf{k}_j \downarrow}^\dagger |0\rangle. \end{aligned} \quad (\text{A2b})$$

For large n such that $\sqrt{n} \gg \alpha$, we can define a new variable $n' = \sqrt{n}/\alpha \approx \sqrt{n-1}/\alpha$, so the term inside the bracket of eq. (A2b) can be rewritten as

$$\begin{aligned} &\frac{\alpha}{\sqrt{n-1} + \alpha} \sum_{j=0}^{\sqrt{n-1}/\alpha} e^{i(m-N)\phi_j} \\ &= \frac{\alpha}{\sqrt{n-1} + \alpha} \sum_{j=0}^{\sqrt{n-1}/\alpha} e^{i(m-N)(-\pi + 2\pi\alpha j/\sqrt{n})}, \\ &\approx \frac{1}{n' + 1} \sum_{j=0}^{n'} e^{i(m-N)(-\pi + 2\pi j/n')}, \\ &= e^{-\pi i(m-N)} \cdot \frac{1}{n' + 1} \sum_{j=0}^{n'} e^{2\pi i(m-N)j/n'}. \end{aligned}$$

Applying the infinite approximation $n \rightarrow \infty$, and thus

$n' \rightarrow \infty$, we have

$$\begin{aligned} &\lim_{n \rightarrow \infty} \frac{\alpha}{\sqrt{n-1} + \alpha} \sum_{j=0}^{\sqrt{n-1}/\alpha} e^{i(m-N)\phi_j} \\ &= e^{-\pi i(m-N)} \lim_{n' \rightarrow \infty} \frac{1}{n' + 1} \sum_{j=0}^{n'} e^{2\pi i(m-N)j/n'}, \\ &\approx e^{-\pi i(m-N)} \cdot \underbrace{\lim_{n' \rightarrow \infty} \frac{1}{n'} \sum_{j=0}^{n'} e^{2\pi i(m-N)j/n'}}_{=\delta_{mN}}, \\ &= e^{-\pi i(m-N)} \delta_{mN} \end{aligned}$$

The Kronecker delta δ_{mN} equals to one at $m = N$ and is zero elsewhere. Now eq. (A2b) is

$$\begin{aligned} |\Psi(N)\rangle &= \left(\frac{\alpha}{\sqrt{n-1} + \alpha} \right)^{-1/2} \sum_{m=0}^n e^{-\pi i(m-N)} \delta_{mN} \sum_{\chi \in \mathcal{S}_m} \\ &\quad \times \prod_{\mathbf{k}_i \in \chi^c} u_{\mathbf{k}_i} \prod_{\mathbf{k}_j \in \chi} v_{\mathbf{k}_j} c_{\mathbf{k}_j \uparrow}^\dagger c_{-\mathbf{k}_j \downarrow}^\dagger |0\rangle, \\ &= \left(\frac{\alpha}{\sqrt{n-1} + \alpha} \right)^{-1/2} \sum_{\chi \in \mathcal{S}_N} \\ &\quad \times \prod_{\mathbf{k}_i \in \chi^c} u_{\mathbf{k}_i} \prod_{\mathbf{k}_j \in \chi} v_{\mathbf{k}_j} c_{\mathbf{k}_j \uparrow}^\dagger c_{-\mathbf{k}_j \downarrow}^\dagger |0\rangle. \end{aligned} \quad (\text{A3})$$

Next, with eq. (A3), the electron number operator \hat{N}^e of a single superconductor acting on this number state $|\Psi(N)\rangle$ gives

$$\begin{aligned}
\hat{N}^e |\Psi(N)\rangle &= \sum_{\mathbf{k}} (c_{\mathbf{k}\uparrow}^\dagger c_{\mathbf{k}\uparrow} + c_{-\mathbf{k}\downarrow}^\dagger c_{-\mathbf{k}\downarrow}) \left(\frac{\alpha}{\sqrt{n-1} + \alpha} \right)^{-1/2} \sum_{\chi \in \mathcal{S}_N} \prod_{\mathbf{k}_i \in \chi^c} u_{\mathbf{k}_i} \prod_{\mathbf{k}_j \in \chi} v_{\mathbf{k}_j} c_{\mathbf{k}_j\uparrow}^\dagger c_{-\mathbf{k}_j\downarrow}^\dagger |0\rangle, \\
&= \left(\frac{\alpha}{\sqrt{n-1} + \alpha} \right)^{-1/2} \sum_{\mathbf{k} \in \chi} \sum_{\chi \in \mathcal{S}_N} \prod_{\mathbf{k}_i \in \chi^c} u_{\mathbf{k}_i} (c_{\mathbf{k}\uparrow}^\dagger c_{\mathbf{k}\uparrow} + c_{-\mathbf{k}\downarrow}^\dagger c_{-\mathbf{k}\downarrow}) \prod_{\mathbf{k}_j \in \chi} v_{\mathbf{k}_j} c_{\mathbf{k}_j\uparrow}^\dagger c_{-\mathbf{k}_j\downarrow}^\dagger |0\rangle, \\
&= \left(\frac{\alpha}{\sqrt{n-1} + \alpha} \right)^{-1/2} \sum_{\mathbf{k} \in \chi} \sum_{\chi \in \mathcal{S}_N} \prod_{\mathbf{k}_i \in \chi^c} u_{\mathbf{k}_i} 2 \prod_{\mathbf{k}_j \in \chi} v_{\mathbf{k}_j} c_{\mathbf{k}_j\uparrow}^\dagger c_{-\mathbf{k}_j\downarrow}^\dagger |0\rangle, \\
&= 2 \sum_{\mathbf{k} \in \chi} 1 \cdot \left(\frac{\alpha}{\sqrt{n-1} + \alpha} \right)^{1/2} \sum_{\chi \in \mathcal{S}_N} \prod_{\mathbf{k}_i \in \chi^c} u_{\mathbf{k}_i} \prod_{\mathbf{k}_j \in \chi} v_{\mathbf{k}_j} c_{\mathbf{k}_j\uparrow}^\dagger c_{-\mathbf{k}_j\downarrow}^\dagger |0\rangle, \\
&= 2N |\Psi(N)\rangle, \quad \because |\chi| = N.
\end{aligned} \tag{A4}$$

The eigenvalue equation $\hat{N}^e |\Psi(N)\rangle = 2N |\Psi(N)\rangle$ implies that we have exactly $2N$ electron in the state $|\Psi(N)\rangle$. This number state is actually that of the Copper pairs:

$$\hat{N}^e = 2\hat{N}.$$

□

Appendix B: Matrix Elements of Superconducting Island Hamiltonian

The matrix elements of the island Hamiltonian projecting onto the low-energy Hilbert space is given by three momentum sums, which can be approximated by the integrals: $\sum_{\mathbf{k}=-\infty}^{\infty} \rightarrow \int_{\Delta}^{b\Delta} dE \rho(E)$, where $\rho(E) = \frac{n}{2\Delta\sqrt{b^2-1}} \frac{E}{\sqrt{E^2-\Delta^2}}$. The matrix elements of PH_lP are given by

$$\begin{aligned}
\langle \Psi(\phi_j) | H_l | \Psi(\phi_{j'}) \rangle &= 2 \sum_{\mathbf{k}_l} \frac{(\epsilon_{\mathbf{k}_l} - \mu_l) v_{\mathbf{k}_l}^2}{u_{\mathbf{k}_l}^2 + v_{\mathbf{k}_l}^2 e^{i\varphi}} - |g|^2 \left(\sum_{\mathbf{k}_l} \frac{u_{\mathbf{k}_l} v_{\mathbf{k}_l}}{u_{\mathbf{k}_l}^2 + v_{\mathbf{k}_l}^2 e^{i\varphi}} \right)^2, \\
&= \sum_{\mathbf{k}_l} \frac{\sqrt{E_{\mathbf{k}_l}^2 - \Delta^2} (E_{\mathbf{k}_l} - \sqrt{E_{\mathbf{k}_l}^2 - \Delta^2})}{E_{\mathbf{k}_l} (1 + e^{i\varphi}) + \sqrt{E_{\mathbf{k}_l}^2 - \Delta^2} (1 - e^{i\varphi})} - |g|^2 \left(\Delta \sum_{\mathbf{k}_l} \frac{1}{E_{\mathbf{k}_l} (1 + e^{i\varphi}) + \sqrt{E_{\mathbf{k}_l}^2 - \Delta^2} (1 - e^{i\varphi})} \right)^2, \\
&\approx \frac{n}{2\Delta\sqrt{b^2-1}} \int_{\Delta}^{b\Delta} \frac{dE}{\sqrt{E^2 - \Delta^2}} \frac{\sqrt{E^2 - \Delta^2} (E - \sqrt{E^2 - \Delta^2})}{(1 + e^{i\varphi}) + \sqrt{E^2 - \Delta^2} (1 - e^{i\varphi})} \\
&\quad - |g|^2 \left(\frac{n}{2\sqrt{b^2-1}} \int_{\Delta}^{b\Delta} \frac{E}{\sqrt{E^2 - \Delta^2}} \frac{dE}{E(1 + e^{i\varphi}) + \sqrt{E^2 - \Delta^2} (1 - e^{i\varphi})} \right)^2, \\
&\equiv \mathcal{K}(\varphi) - |g|^2 \mathcal{V}(\varphi),
\end{aligned} \tag{B1}$$

where $\varphi \equiv \phi_{j'} - \phi_j$. The complex functions $\mathcal{K}(\varphi)$ and $\mathcal{V}(\varphi)$ are

$$\begin{aligned}
\mathcal{K}(\varphi) &= \frac{-1}{4\sqrt{b^2-1}} e^{-i\varphi} n \Delta \left\{ b \left(\sqrt{b^2-1} - b \right) + \cos \varphi \ln \left(b - \sqrt{b^2-1} \right) + 1 \right. \\
&\quad \left. + i \sin \varphi \left[\ln \left(b - \sqrt{b^2-1} \right) - \ln \left(e^{i\varphi} \left(2b(\sqrt{b^2-1} - b) + 1 \right) - 1 \right) - 2 \ln \Delta + \ln(-\Delta^2(e^{i\varphi} + 1)) \right] \right\}, \tag{B2}
\end{aligned}$$

$$\begin{aligned}
\mathcal{V}(\varphi) &= \frac{n^2}{16(b^2-1)} \left\{ -2 \ln \left(b - \sqrt{b^2-1} \right) \right. \\
&\quad \left. + e^{-i\varphi} (e^{i\varphi} - 1) \left[\ln \left(e^{i\varphi} \left(1 + 2b(\sqrt{b^2-1} - b) \right) - 1 \right) - \ln(-1 - e^{i\varphi}) \right] \right\}^2. \tag{B3}
\end{aligned}$$

Appendix C: Josephson Effect & Greens' Functions

We apply the concept of Greens' functions for the calculations in the second-order perturbation term. For

a given diagonalisable Hamiltonian, the Fourier's trans-

form of its propagator relates to its Hamiltonian inverse. Therefore,

$$H_T \frac{1}{E_0 \bar{P} - \bar{P} H_0 \bar{P}} H_T D_\varphi = \mathcal{F}_{\tau \rightarrow E_0} [H_T U_0(\tau) H_T D_\varphi],$$

where $U_0(\tau)$ is the propagator for H_0 at time τ . The matrix elements of the projection in eq. (54) is then the Fourier's transformation of the expectation value:

$$\langle \Psi(\phi_j) | H_T (E_0 \bar{P} - \bar{P} H_0 \bar{P})^{-1} H_T D_\varphi | \Psi(\phi_j) \rangle = \mathcal{F}_{\tau \rightarrow E_0} \langle H_T U_0(\tau) H_T D_\varphi \rangle. \quad (\text{C1})$$

The expectation value on the right-hand side is taken with respect to the BCS ground state:

$$\begin{aligned} \langle H_T(\tau) H_T D_\varphi \rangle &= \langle \Psi(\phi_j) | H_T(\tau) H_T D_\varphi | \Psi(\phi_j) \rangle, \\ &= \langle \Psi(\phi_j) | U_0^\dagger(\tau) H_T U_0(\tau) H_T D_\varphi | \Psi(\phi_j) \rangle, \\ &= e^{i E_0 \tau} \langle \Psi(\phi_j) | H_T U_0(\tau) H_T D_\varphi | \Psi(\phi_j) \rangle, \end{aligned}$$

so

$$\langle H_T U_0(\tau) H_T D_\varphi \rangle = e^{-i E_0 \tau} \langle \Psi(\phi_j) | H_T(\tau) H_T D_\varphi | \Psi(\phi_j) \rangle. \quad (\text{C2})$$

Taking the Fourier's transform on the both sides,

$$\begin{aligned} \mathcal{F}_{\tau \rightarrow E_0} [\langle \Psi(\phi_j) | H_T U_0(\tau) H_T | \Psi(\phi_j) \rangle] &= \mathcal{F}_{\tau \rightarrow E_0} [e^{-i E_0 \tau} \langle \Psi(\phi_j) | H_T(\tau) H_T D_\varphi | \Psi(\phi_j) \rangle], \\ &= \mathcal{F}_{\tau \rightarrow E_0} [\langle \Psi(\phi_j) | U_0(\tau) H_T(\tau) H_T D_\varphi | \Psi(\phi_j) \rangle], \\ &= \mathcal{F}_{\tau \rightarrow E_0} [\langle \Psi(\phi_j) | \mathcal{T}_\tau (H_T(\tau) H_T D_\varphi) | \Psi(\phi_j) \rangle], \\ &= \mathcal{F}_{\tau \rightarrow E_0} [\mathcal{T}_\tau \langle H_T(\tau) H_T D_\varphi \rangle], \end{aligned} \quad (\text{C3})$$

□

i.e., the matrix elements are the Fourier's transform of the Greens' functions $\mathcal{F}_{\tau \rightarrow E_0} \langle \mathcal{T}_\tau (H_T(\tau) H_T D_\varphi) \rangle$.

Proof. The propagator $U_0(\tau)$ can be expanded as the time ordering sequence

$$\begin{aligned} U_0(\tau) &= \mathcal{T}_\tau \exp \left(\frac{-i}{\hbar} \int_0^\tau dt H_0(t) \right), \\ &= \mathcal{T}_\tau \left(\mathbb{I} - \frac{i}{\hbar} \int_0^\tau dt H_0(t) + \dots \right), \end{aligned}$$

such that

$$\begin{aligned} U_0(\tau) H_T(\tau) H_T D_\varphi &= \mathcal{T}_\tau (H_T(\tau) H_T D_\varphi) \\ &\quad - \frac{i}{\hbar} \int_0^\tau dt H_0(t) H_T(\tau) H_T D_\varphi \\ &\quad + \dots, \\ &\approx \mathcal{T}_\tau (H_T(\tau) H_T D_\varphi). \end{aligned}$$

Expanding the time-ordering product in eq. (C3) and applying Wick's theorem to factorise the correlation functions, we have

$$\begin{aligned} \langle \mathcal{T}_\tau c_{\mathbf{k}_A s}^\dagger(\tau) c_{\mathbf{k}_B s}(\tau) c_{\mathbf{k}_A \sigma}^\dagger c_{\mathbf{k}_B \sigma} D_{\varphi_A} D_{\varphi_B} \rangle &= \theta(\tau) \langle c_{\mathbf{k}_A s}^\dagger(\tau) c_{\mathbf{k}_B s}(\tau) c_{\mathbf{k}_A \sigma}^\dagger c_{\mathbf{k}_B \sigma} D_{\varphi_A} D_{\varphi_B} \rangle \\ &\quad - \theta(-\tau) \langle c_{\mathbf{k}_A \sigma}^\dagger c_{\mathbf{k}_B \sigma} D_{\varphi_A} D_{\varphi_B} c_{\mathbf{k}_A s}^\dagger(\tau) c_{\mathbf{k}_B s}(\tau) \rangle, \\ &= 2\theta(\tau) \langle c_{\mathbf{k}_A s}^\dagger(\tau) c_{\mathbf{k}_A \sigma}^\dagger D_{\varphi_A} \rangle \langle c_{\mathbf{k}_B s}(\tau) c_{\mathbf{k}_B \sigma} D_{\varphi_B} \rangle \end{aligned} \quad (\text{C4a})$$

$$\begin{aligned} &\quad - 2\theta(-\tau) \langle c_{\mathbf{k}_A \sigma}^\dagger D_{\varphi_A} c_{\mathbf{k}_A s}^\dagger(\tau) \rangle \langle c_{\mathbf{k}_B \sigma} D_{\varphi_B} c_{\mathbf{k}_B s}(\tau) \rangle, \\ &= 2 \langle \mathcal{T}_\tau c_{\mathbf{k}_A s}^\dagger(\tau) c_{\mathbf{k}_A \sigma}^\dagger D_{\varphi_A} \rangle \langle \mathcal{T}_\tau c_{\mathbf{k}_B \sigma} D_{\varphi_B} c_{\mathbf{k}_B s}(\tau) \rangle, \\ &= 2 \langle \mathcal{T}_\tau c_{\mathbf{k}_A s}^\dagger(\tau) c_{\mathbf{k}_A \sigma}^\dagger D_{\varphi_A} \rangle \langle \mathcal{T}_\tau c_{\mathbf{k}_B \sigma}(-\tau) c_{\mathbf{k}_B s} D_{\varphi_B} \rangle, \end{aligned} \quad (\text{C4b})$$

where subscripts s, σ denote the spin indices, and the expectation values are taken with respect to $|\Psi(\phi_j)\rangle$. With the factorisation of the expectation value (proved in Section C1)

$$\langle c_{\mathbf{k}_A s}^\dagger(\tau) c_{\mathbf{k}_A \sigma}^\dagger (N_A^e)^n \rangle = \langle c_{\mathbf{k}_A s}^\dagger(\tau) c_{\mathbf{k}_A \sigma}^\dagger \rangle \langle (N_A^e)^n \rangle, \quad (\text{C5})$$

and the BCS overlap expressed with the phase displace-

ment operator

$$\sum_n \frac{(i\varphi)^n}{n!} \langle (N^e)^n \rangle = \mathcal{W}(\varphi) \quad \varphi = \phi' - \phi, \quad (\text{C6})$$

we expand the phase displacement operator in the first

term in eq. (C4b) by Taylor's series as

$$\begin{aligned} \langle \mathcal{T}_\tau c_{\mathbf{k}_A s}^\dagger(\tau) c_{\mathbf{k}_A \sigma}^\dagger D_{\varphi_A} \rangle &= \left\langle c_{\mathbf{k}_A s}^\dagger(\tau) c_{\mathbf{k}_A \sigma}^\dagger \right\rangle + (i\varphi_A/2) \left\langle c_{\mathbf{k}_A s}^\dagger(\tau) c_{\mathbf{k}_A \sigma}^\dagger (2N_A^e) \right\rangle \\ &\quad + \frac{(i\varphi_A/2)^2}{2!} \left\langle c_{\mathbf{k}_A s}^\dagger(\tau) c_{\mathbf{k}_A \sigma}^\dagger (2N_A^e)^2 \right\rangle + \dots, \end{aligned} \quad (\text{C7a})$$

$$\begin{aligned} &= \left\langle c_{\mathbf{k}_A s}^\dagger(\tau) c_{\mathbf{k}_A \sigma}^\dagger \right\rangle + (i\varphi_A) \left\langle c_{\mathbf{k}_A s}^\dagger(\tau) c_{\mathbf{k}_A \sigma}^\dagger N_A^e \right\rangle \\ &\quad + \frac{(i\varphi_A)^2}{2!} \left\langle c_{\mathbf{k}_A s}^\dagger(\tau) c_{\mathbf{k}_A \sigma}^\dagger (N_A^e)^2 \right\rangle + \dots, \end{aligned} \quad (\text{C7a})$$

$$\begin{aligned} &= \left\langle c_{\mathbf{k}_A s}^\dagger(\tau) c_{\mathbf{k}_A \sigma}^\dagger N_A^e \right\rangle \\ &\quad \cdot \left(1 + (i\varphi_A) \langle N_A^e \rangle + \frac{(i\varphi_A)^2}{2!} \langle (N_A^e)^2 \rangle + \dots \right), \quad (\text{C7b}) \end{aligned}$$

$$= \left\langle c_{\mathbf{k}_A s}^\dagger(\tau) c_{\mathbf{k}_A \sigma}^\dagger \right\rangle \mathcal{W}(\varphi_A), \quad (\text{C7c})$$

where $\mathcal{W}(\varphi_A) = \langle \Psi_A(\phi_j) | \Psi_A(\phi_{j'}) \rangle$ is the overlap function of the BCS ground state for island A . Similarly for island B :

$$\langle \mathcal{T}_\tau c_{\mathbf{k}_B s}(-\tau) c_{\mathbf{k}_B s} D_{\varphi_B} \rangle = \langle c_{\mathbf{k}_B s}(-\tau) c_{\mathbf{k}_B s} \rangle \mathcal{W}(\varphi_B).$$

Proof. We have computed the BCS overlap function $\mathcal{W}(\varphi)$ directly from the definition in Section II C. Here with the introduction of the phase displacement operator D_φ , we will do the inner product again to obtain the deeply insight. The overlap now becomes the expectation

value of D_φ :

$$\mathcal{W}(\varphi) = \langle \Psi(\phi_j) | \Psi(\phi_{j'}) \rangle = \langle \Psi(\phi_j) | D_\varphi | \Psi(\phi_j) \rangle \quad (\text{C8a})$$

$$\begin{aligned} &= \langle 0 | \prod_{\mathbf{q}'} (u_{\mathbf{q}'} + v_{\mathbf{q}'} e^{-i\phi_j} c_{-\mathbf{q}'\downarrow} c_{\mathbf{q}'\uparrow}) \\ &\quad \times \left[\mathbb{I} + (i\varphi/2) \left(\sum_{\mathbf{k}} c_{\mathbf{k}\uparrow}^\dagger c_{\mathbf{k}\uparrow} + c_{-\mathbf{k}\downarrow}^\dagger c_{-\mathbf{k}\downarrow} \right) + \dots \right] \\ &\quad \times \prod_{\mathbf{q}'} (u_{\mathbf{q}'} + v_{\mathbf{q}'} e^{i\phi_{j'}} c_{\mathbf{q}'\uparrow}^\dagger c_{-\mathbf{q}'\downarrow}^\dagger) | 0 \rangle, \end{aligned}$$

$$= 1 + (i\varphi/2) \langle N \rangle + \frac{(i\varphi/2)^2}{2!} \langle N^2 \rangle + \dots, \quad (\text{C8b})$$

$$\begin{aligned} &= 1 + (i\varphi) \langle N^e \rangle + \frac{(i\varphi)^2}{2!} \langle (N^e)^2 \rangle + \dots, \quad (\text{C8b}) \\ &= \sum_{n=0}^{\infty} \frac{(i\varphi)^n}{n!} \langle (N^e)^n \rangle, \quad (\text{C8c}) \end{aligned}$$

$$= \langle e^{i\varphi \hat{N}^e} \rangle, \quad (\text{C8d})$$

i.e., we can express $\mathcal{W}(\varphi)$ as the expectation value of D_φ . \square

Hence, by taking the tunneling matrix element as a constant $t_{\mathbf{k}_A \mathbf{k}_B} \approx t$ [37], a convenient approximation for a symmetric junction, we obtain

$$\begin{aligned} \langle \mathcal{T}_\tau H_T(\tau) H_T D_\varphi \rangle &= 2 \sum_{\mathbf{k}_A \mathbf{k}_B s \sigma} e^{i\phi_j} t_{\mathbf{k}_A \mathbf{k}_B}^2 \left\langle \mathcal{T}_\tau c_{\mathbf{k}_A s}^\dagger(\tau) c_{\mathbf{k}_A \sigma}^\dagger \right\rangle \langle \mathcal{T}_\tau c_{\mathbf{k}_B s}(-\tau) c_{\mathbf{k}_B s} \rangle J(\varphi_A) J(\varphi_B) + c.c., \\ &= 2 \sum_{\mathbf{k}_A \mathbf{k}_B s \sigma} e^{i\phi_j} t_{\mathbf{k}_A \mathbf{k}_B}^2 \left\langle \mathcal{T}_\tau c_{\mathbf{k}_A s}^\dagger(\tau) c_{\mathbf{k}_A \sigma}^\dagger \right\rangle \langle \mathcal{T}_\tau c_{\mathbf{k}_B s}(-\tau) c_{\mathbf{k}_A s} \rangle J(\varphi) + c.c., \\ &= 2e^{i\phi_j} \sum_{\mathbf{k}_A \mathbf{k}_B s \sigma} t_{\mathbf{k}_A \mathbf{k}_B}^2 \mathcal{F}_{s\sigma}(\mathbf{k}_A, \tau) \mathcal{F}_{s\sigma}^*(\mathbf{k}_B, -\tau) \langle \Psi(\phi_j) | \Psi(\phi_{j'}) \rangle + c.c., \\ &= 2e^{i\phi_j} \sum_{\mathbf{k}_A \mathbf{k}_B} t_{\mathbf{k}_A \mathbf{k}_B}^2 \mathcal{F}_{\uparrow\downarrow}(\mathbf{k}_A, \tau) \mathcal{F}_{\uparrow\downarrow}^*(\mathbf{k}_B, -\tau) \langle \Psi(\phi_j) | \Psi(\phi_{j'}) \rangle + c.c., \\ &\approx 2e^{i\phi_j} t^2 \sum_{\mathbf{k}_A \mathbf{k}_B} \mathcal{F}_{\uparrow\downarrow}(\mathbf{k}_A, \tau) \mathcal{F}_{\uparrow\downarrow}^*(\mathbf{k}_B, -\tau) \langle \Psi(\phi_j) | \Psi(\phi_{j'}) \rangle + c.c., \end{aligned} \quad (\text{C9})$$

which is provided in eq. (54). Note that the anomalous Greens' functions $\mathcal{F}_{\uparrow\uparrow} = \mathcal{F}_{\downarrow\downarrow} = 0$.

Proof. Here we show that the anomalous Greens' functions $\mathcal{F}_{ss} = 0$. For simplicity, we consider only a single mode existing on the given superconductor. By Bogoliubov transformation

$$\begin{pmatrix} b_{\mathbf{k}\uparrow}^\dagger \\ b_{-\mathbf{k}\downarrow} \end{pmatrix} = \begin{pmatrix} u_{\mathbf{k}} & -v_{\mathbf{k}} e^{-i\phi} \\ v_{\mathbf{k}} e^{i\phi} & u_{\mathbf{k}} \end{pmatrix} \begin{pmatrix} c_{\mathbf{k}\uparrow}^\dagger \\ c_{-\mathbf{k}\downarrow} \end{pmatrix}. \quad (\text{C10})$$

the time-dependent fermionic annihilation operator is

given by

$$c_{\mathbf{k}_l \uparrow}(\tau) = e^{H_l \tau} \left(u_{\mathbf{k}_l} b_{\mathbf{k}_l \uparrow} + v_{\mathbf{k}_l} e^{i\phi} b_{-\mathbf{k}_l \downarrow}^\dagger \right) e^{-H_l \tau}, \quad (\text{C11a})$$

$$= u_{\mathbf{k}_l} b_{\mathbf{k}_l \uparrow} e^{-E_{\mathbf{k}_l} \tau} + v_{\mathbf{k}_l} e^{i\phi} b_{-\mathbf{k}_l \downarrow}^\dagger e^{E_{\mathbf{k}_l} \tau},$$

$$= u_{\mathbf{k}_l} \left(u_{\mathbf{k}_l} c_{\mathbf{k}_l \uparrow} - v_{\mathbf{k}_l} e^{i\phi} c_{-\mathbf{k}_l \downarrow}^\dagger \right) e^{-E_{\mathbf{k}_l} \tau}$$

$$+ v_{\mathbf{k}_l} e^{i\phi} \left(v_{\mathbf{k}_l} e^{-i\phi} c_{\mathbf{k}_l \uparrow} + u_{\mathbf{k}_l} c_{-\mathbf{k}_l \downarrow}^\dagger \right) e^{E_{\mathbf{k}_l} \tau},$$

$$= (u_{\mathbf{k}_l}^2 e^{-E_{\mathbf{k}_l} \tau} + v_{\mathbf{k}_l}^2 e^{E_{\mathbf{k}_l} \tau}) c_{\mathbf{k}_l \uparrow} + u_{\mathbf{k}_l} v_{\mathbf{k}_l} e^{i\phi} (e^{E_{\mathbf{k}_l} \tau} - e^{-E_{\mathbf{k}_l} \tau}) c_{-\mathbf{k}_l \downarrow}^\dagger. \quad (\text{C11b})$$

H_l is the superconductor Hamiltonian for the island l . The Greens' functions are then

$$\langle c_{\mathbf{k}_l\uparrow}(\tau)c_{\mathbf{k}_l\uparrow} \rangle = \left(u_{\mathbf{k}_l}^2 e^{-E_{\mathbf{k}_l}\tau} + v_{\mathbf{k}_l}^2 e^{E_{\mathbf{k}_l}\tau} \right) \overbrace{\langle c_{\mathbf{k}_l\uparrow} c_{\mathbf{k}_l\uparrow} \rangle}^0 + u_{\mathbf{k}_l} v_{\mathbf{k}_l} e^{i\phi} \left(e^{E_{\mathbf{k}_l}\tau} - e^{-E_{\mathbf{k}_l}\tau} \right) \overbrace{\langle c_{-\mathbf{k}_l\downarrow} c_{-\mathbf{k}_l\downarrow}^\dagger \rangle}^0, \quad (C12)$$

$$= 0, \quad (C13)$$

$$\langle c_{\mathbf{k}_l\uparrow} c_{\mathbf{k}_l\uparrow}(\tau) \rangle = 0. \quad (C14)$$

The result can be generalised to the spin-down case:

$$\langle c_{-\mathbf{k}_l\downarrow}(\tau)c_{-\mathbf{k}_l\downarrow} \rangle = \langle c_{-\mathbf{k}_l\downarrow} c_{-\mathbf{k}_l\downarrow}(\tau) \rangle = 0.$$

The electron mode \mathbf{k} can be arbitrary. Therefore,

$$\mathcal{F}_{ss} \equiv \theta(\tau) \langle c_{\mathbf{k}s}(\tau)c_{\mathbf{k}s} \rangle - \theta(-\tau) \langle c_{\mathbf{k}s} c_{\mathbf{k}s}(\tau) \rangle = 0, \quad (C14)$$

the anomalous Greens' functions with the identical spin indices are zeros: $\mathcal{F}_{\uparrow\uparrow} = \mathcal{F}_{\downarrow\downarrow} = 0$. \square

1. Factorisation in Greens' Functions

We prove eq. (C5) here. The expectation value $\langle (N^e)^n \rangle$ is given by

$$\begin{aligned} \langle (N^e)^n \rangle &= \langle 0 | \prod_{\mathbf{q}'} (u_{\mathbf{q}'} + v_{\mathbf{q}'} e^{-i\phi_j} c_{-\mathbf{q}'\downarrow} c_{\mathbf{q}'\uparrow}) \left(\sum_{\mathbf{k}} c_{\mathbf{k}\uparrow}^\dagger c_{\mathbf{k}\uparrow} + c_{-\mathbf{k}\downarrow}^\dagger c_{-\mathbf{k}\downarrow} \right)^n \prod_{\mathbf{q}'} (u_{\mathbf{q}'} + v_{\mathbf{q}'} e^{i\phi_j} c_{\mathbf{q}'\uparrow}^\dagger c_{-\mathbf{q}'\downarrow}) | 0 \rangle, \\ &= 2^n \sum_{\mathbf{k}} \langle 0 | \prod_{\mathbf{q}\mathbf{q}'} (u_{\mathbf{q}'} + v_{\mathbf{q}'} e^{-i\phi_j} c_{-\mathbf{q}'\downarrow} c_{\mathbf{q}'\uparrow}) \\ &\quad \times \left\{ \left(c_{\mathbf{k}\uparrow}^\dagger c_{\mathbf{k}\uparrow} \right)^n + \left(\sum_{\mathbf{k}_1 \neq \mathbf{k}} c_{\mathbf{k}_1\uparrow}^\dagger c_{\mathbf{k}_1\uparrow} c_{\mathbf{k}\uparrow}^\dagger c_{\mathbf{k}\uparrow} \cdots c_{\mathbf{k}\uparrow}^\dagger c_{\mathbf{k}\uparrow} \right) + \left(\sum_{\mathbf{k}_2 \neq \mathbf{k}} c_{\mathbf{k}_2\uparrow}^\dagger c_{\mathbf{k}_2\uparrow} c_{\mathbf{k}_2\uparrow}^\dagger c_{\mathbf{k}_2\uparrow} \cdots c_{\mathbf{k}\uparrow}^\dagger c_{\mathbf{k}\uparrow} \right) + \cdots \right\} \\ &\quad \times (u_{\mathbf{q}} + v_{\mathbf{q}} e^{i\phi_j} c_{\mathbf{q}\uparrow}^\dagger c_{-\mathbf{q}\downarrow}) | 0 \rangle, \\ &= 2^n \sum_{\mathbf{k}} \left(v_{\mathbf{k}}^{2n} + \sum_{\mathbf{k}_1 \neq \mathbf{k}} v_{\mathbf{k}_1}^2 \underbrace{v_{\mathbf{k}}^2 \cdots v_{\mathbf{k}}^2}_{n-1} + \sum_{\mathbf{k}_2 \neq \mathbf{k}} v_{\mathbf{k}_2}^2 v_{\mathbf{k}_2}^2 \underbrace{\cdots v_{\mathbf{k}}^2}_{n-2} + \cdots \right). \end{aligned} \quad (C15)$$

On the other hand, the correlation functions are

$$\langle c_{\mathbf{k}\uparrow}^\dagger(\tau) c_{\mathbf{k}\uparrow}^\dagger \rangle = \mathcal{F}_{\uparrow\uparrow}^* = 0, \quad (C16a)$$

$$\langle c_{-\mathbf{k}\downarrow}^\dagger(\tau) c_{-\mathbf{k}\downarrow}^\dagger \rangle = \mathcal{F}_{\downarrow\downarrow}^* = 0, \quad (C16b)$$

$$\langle c_{\mathbf{k}\uparrow}^\dagger(\tau) c_{-\mathbf{k}\downarrow}^\dagger \rangle = \mathcal{F}_{\uparrow\downarrow} = u_{\mathbf{k}} v_{\mathbf{k}}^3 (e^{E_{\mathbf{k}}\tau} - e^{-E_{\mathbf{k}}\tau}), \quad (C16c)$$

$$\langle c_{-\mathbf{k}\downarrow}^\dagger(\tau) c_{\mathbf{k}\uparrow}^\dagger \rangle = \mathcal{F}_{\downarrow\uparrow} = u_{\mathbf{k}} v_{\mathbf{k}}^3 (e^{E_{\mathbf{k}}\tau} - e^{-E_{\mathbf{k}}\tau}). \quad (C16d)$$

The left-hand side of eq. (C5) is discussed separately. For $s \neq \sigma$, we have

$$\begin{aligned}
\left\langle c_{\mathbf{k}s}^\dagger(\tau)c_{\mathbf{k}\sigma}^\dagger(N^e)^n \right\rangle &= 2^n \sum_{\mathbf{k}} \left\langle c_{\mathbf{k}s}^\dagger(\tau)c_{\mathbf{k}\sigma}^\dagger \left(c_{\mathbf{k}\uparrow}^\dagger c_{\mathbf{k}\uparrow} \right)^n \right\rangle + \left\langle c_{\mathbf{k}s}^\dagger(\tau)c_{\mathbf{k}\sigma}^\dagger \left(\sum_{\mathbf{k}_1 \neq \mathbf{k}} c_{\mathbf{k}_1\uparrow}^\dagger c_{\mathbf{k}_1\uparrow} c_{\mathbf{k}\uparrow}^\dagger c_{\mathbf{k}\uparrow} \cdots c_{\mathbf{k}\uparrow}^\dagger c_{\mathbf{k}\uparrow} \right) \right\rangle + \cdots, \\
&= 2^n \sum_{\mathbf{k}} (u_{\mathbf{k}}^2 e^{-E_{\mathbf{k}\tau}} + v_{\mathbf{k}}^2 e^{E_{\mathbf{k}\tau}}) \underbrace{\left\langle c_{\mathbf{k}s}^\dagger c_{\mathbf{k}\sigma}^\dagger \left(c_{\mathbf{k}\uparrow}^\dagger c_{\mathbf{k}\uparrow} \right)^n \right\rangle}_0 \\
&\quad + u_{\mathbf{k}} v_{\mathbf{k}}^3 (e^{E_{\mathbf{k}\tau}} - e^{-E_{\mathbf{k}\tau}}) \left\langle c_{\mathbf{k}\sigma}^\dagger c_{\mathbf{k}\sigma}^\dagger \left(c_{\mathbf{k}\uparrow}^\dagger c_{\mathbf{k}\uparrow} \right)^n \right\rangle \\
&\quad + (u_{\mathbf{k}}^2 e^{-E_{\mathbf{k}\tau}} + v_{\mathbf{k}}^2 e^{E_{\mathbf{k}\tau}}) \underbrace{\left\langle c_{\mathbf{k}s}^\dagger c_{\mathbf{k}\sigma}^\dagger \sum_{\mathbf{k}_1 \neq \mathbf{k}} c_{\mathbf{k}_1\uparrow}^\dagger c_{\mathbf{k}_1\uparrow} c_{\mathbf{k}\uparrow}^\dagger c_{\mathbf{k}\uparrow} \cdots c_{\mathbf{k}\uparrow}^\dagger c_{\mathbf{k}\uparrow} \right\rangle}_0 \\
&\quad + u_{\mathbf{k}} v_{\mathbf{k}}^3 (e^{E_{\mathbf{k}\tau}} - e^{-E_{\mathbf{k}\tau}}) \underbrace{\left\langle c_{\mathbf{k}s}^\dagger c_{\mathbf{k}\sigma}^\dagger \sum_{\mathbf{k}_1 \neq \mathbf{k}} c_{\mathbf{k}_1\uparrow}^\dagger c_{\mathbf{k}_1\uparrow} c_{\mathbf{k}\uparrow}^\dagger c_{\mathbf{k}\uparrow} \cdots c_{\mathbf{k}\uparrow}^\dagger c_{\mathbf{k}\uparrow} \right\rangle}_0 \\
&\quad + \cdots, \\
&= 2^n u_{\mathbf{k}'} v_{\mathbf{k}'}^3 (e^{E_{\mathbf{k}'\tau}} - e^{-E_{\mathbf{k}'\tau}}) \sum_{\mathbf{k}} \left(v_{\mathbf{k}}^{2n} + \sum_{\mathbf{k}_1 \neq \mathbf{k}} v_{\mathbf{k}_1}^2 v_{\mathbf{k}}^2 \cdots v_{\mathbf{k}}^2 + \cdots \right). \tag{C17}
\end{aligned}$$

However if $s = \sigma$, all the expectation values vanish according to the exclusive principle, such that

$$\left\langle c_{\mathbf{k}s}^\dagger(\tau)c_{\mathbf{k}s}^\dagger(N^e)^n \right\rangle = 0. \tag{C18}$$

Conclusively, combining the results in Eqs. (C15), (C16), (C17), (C18), we obtain

$$\begin{aligned}
\left\langle c_{\mathbf{k}s}^\dagger(\tau)c_{\mathbf{k}\sigma}^\dagger \right\rangle ((N^e)^n) &= \left\langle c_{\mathbf{k}s}^\dagger(\tau)c_{\mathbf{k}\sigma}^\dagger(N^e)^n \right\rangle, \\
&= \begin{cases} 0, & s = \sigma \\ 2^n u_{\mathbf{k}'} v_{\mathbf{k}'}^3 (e^{E_{\mathbf{k}'\tau}} - e^{-E_{\mathbf{k}'\tau}}) \sum_{\mathbf{k}} \left(v_{\mathbf{k}}^{2n} + \sum_{\mathbf{k}_1 \neq \mathbf{k}} v_{\mathbf{k}_1}^2 v_{\mathbf{k}}^2 \cdots v_{\mathbf{k}}^2 + \sum_{\mathbf{k}_2 \neq \mathbf{k}} v_{\mathbf{k}_2}^2 v_{\mathbf{k}_2}^2 \cdots v_{\mathbf{k}}^2 + \cdots \right) & s \neq \sigma \end{cases}. \tag{C19}
\end{aligned}$$

2. Finite-Temperature Fourier Transform

In this section, we compute the matrix elements $\langle \Psi(\phi_j) | H_T(E_0 \bar{P} - \bar{P} H_0 \bar{P})^{-1} H_T | \Psi(\phi_{j'}) \rangle$. Firstly, we take the finite-temperature Fourier transform of eq. (54) [21], to get

$$\begin{aligned}
\mathcal{F}_{\tau \rightarrow E_0} \langle H_T(\tau) H_T D_\varphi \rangle &= 2e^{i\phi_j} t^2 \frac{1}{\beta} \sum_{i\mathcal{E}_n i\mathcal{E}_{n'}} \sum_{\mathbf{k}_A \mathbf{k}_B} \mathcal{F}_{\uparrow\downarrow}(\mathbf{k}_A, i\mathcal{E}_n) \mathcal{F}_{\uparrow\downarrow}^*(\mathbf{k}_B, i\mathcal{E}_{n'}) \underbrace{\frac{1}{\beta} \int_0^\beta d\tau e^{i\tau(\mathcal{E}_{n'} - \mathcal{E}_n + E_0)}}_{=\delta_{\mathcal{E}_{n'}, \mathcal{E}_n - E_0}} \langle \Psi(\phi_j) | \Psi(\phi_{j'}) \rangle, \\
&= 2e^{i\phi_j} t^2 \sum_{\mathbf{k}_A \mathbf{k}_B} \frac{1}{\beta} \sum_{i\mathcal{E}_n} \mathcal{F}_{\uparrow\downarrow}(\mathbf{k}_A, i\mathcal{E}_n) \mathcal{F}_{\uparrow\downarrow}^*(\mathbf{k}_B, i(\mathcal{E}_n - E_0)) \langle \Psi(\phi_j) | \Psi(\phi_{j'}) \rangle + \text{c.c.}, \tag{C20}
\end{aligned}$$

where β is the Boltzmann temperature and E_0 is the eigenenergy of H_0 . We then compute the Matsubara sum by a contour integral [21]:

$$\frac{1}{\beta} \sum_{i\mathcal{E}_n} \mathcal{F}_{\uparrow\downarrow}(\mathbf{k}_A, i\mathcal{E}_n) \mathcal{F}_{\uparrow\downarrow}^*(\mathbf{k}_B, i(\mathcal{E}_n - E_0)) = \frac{1}{\beta} \sum_{i\mathcal{E}_n} \frac{-\Delta}{(i\mathcal{E}_n)^2 - ((\epsilon_{\mathbf{k}_A} - \mu_A)^2 + |\Delta|^2)} \frac{-\Delta}{(i\mathcal{E}_n - iE_0)^2 - ((\epsilon_{\mathbf{k}_B} - \mu_B)^2 + |\Delta|^2)}, \tag{C21a}$$

$$\approx \frac{\Delta^2}{4E_{\mathbf{k}_A} E_{\mathbf{k}_B}} \left(\frac{1}{iE_0 + E_{\mathbf{k}_A} + E_{\mathbf{k}_B}} - \frac{1}{iE_0 - E_{\mathbf{k}_A} - E_{\mathbf{k}_B}} \right), \text{ for } \beta \rightarrow \infty, \tag{C21a}$$

$$= \frac{\Delta^2}{2E_{\mathbf{k}_A} E_{\mathbf{k}_B}} \cdot \frac{E_{\mathbf{k}_A} + E_{\mathbf{k}_B}}{E_0^2 + (E_{\mathbf{k}_A} + E_{\mathbf{k}_B})^2}. \tag{C21b}$$

The residues occurs at the poles $i\mathcal{E}_r = \pm E_{\mathbf{k}_A}, iE_0 \pm E_{\mathbf{k}_B}$. The number of excitation is chosen to be zero as we assume zero temperature $\beta \rightarrow \infty$ in our case. We compute the momentum sum by integral approximation $\sum_{\mathbf{k}=-\infty}^{\infty} \rightarrow \int_0^{b\Delta} dE_{\mathbf{k}} \rho(E_{\mathbf{k}})$. After some algebra given in appendix C3, we obtain

$$\sum_{\mathbf{k}_A \mathbf{k}_B} \frac{1}{\beta} \sum_{i\mathcal{E}_n} \mathcal{F}_{\uparrow\downarrow}(\mathbf{k}_A, i\mathcal{E}_n) \mathcal{F}_{\uparrow\downarrow}^*(\mathbf{k}_B, i(\mathcal{E}_n - E_0)) = \frac{2N_A^e N_B^e}{b^2 - 1} \mathcal{I}(E_0, \Delta). \quad (\text{C22})$$

We evaluate the double integral $\mathcal{I}(E_0, \Delta)$ in appendix C3.

3. Double Integral $\mathcal{I}(E_0, \Delta)$

We approximate the Matsubara sum and the momentum sum in eq. (C22) by a double integral $\mathcal{I}(E_0, \Delta)$:

$$\mathcal{I}(E_0, \Delta) \equiv \int_{\Delta}^{\infty} dE_{\mathbf{k}_A} \int_{\Delta}^{\infty} dE_{\mathbf{k}_B} \frac{E_{\mathbf{k}_A} + E_{\mathbf{k}_B}}{(E_0^2 + (E_{\mathbf{k}_A} + E_{\mathbf{k}_B})^2) \sqrt{(E_{\mathbf{k}_A}^2 - \Delta^2)(E_{\mathbf{k}_B}^2 - \Delta^2)}}, \quad (\text{C23})$$

with the introduction of the density of state in eq. (15). In this appendix, we are going to compute $\mathcal{I}(E_0, \Delta)$ in two limits: (1) $E_0 \ll \Delta$ and (2) $E_0 \gg \Delta$.

a. $E_0 \ll \Delta$

We expand the integral at $E_0 = 0$ for small E_0 case:

$$\begin{aligned} \mathcal{I} &\approx \int_{\Delta}^{\infty} dE_{\mathbf{k}_A} \int_{\Delta}^{\infty} dE_{\mathbf{k}_B} \left(\frac{2}{(E_{\mathbf{k}_A} + E_{\mathbf{k}_B}) \sqrt{(E_{\mathbf{k}_A}^2 - \Delta^2)(E_{\mathbf{k}_B}^2 - \Delta^2)}} - \frac{2E_0^2}{(E_{\mathbf{k}_A} + E_{\mathbf{k}_B})^3 \sqrt{(E_{\mathbf{k}_A}^2 - \Delta^2)(E_{\mathbf{k}_B}^2 - \Delta^2)}} \right) + \mathcal{O}((E_0/\Delta)^4), \\ &= \frac{\pi^2}{2\Delta} - \frac{E_0^2 \pi^2}{32\Delta^3} + \mathcal{O}((E_0/\Delta)^4), \quad \text{for } E_0 \ll \Delta. \end{aligned}$$

So,

$$\mathcal{I}(E_0, \Delta) \approx \frac{\pi^2}{2\Delta} \left(1 - \frac{E_0^2}{16\Delta^2} \right), \quad \text{for } E_0 \ll \Delta. \quad (\text{C24})$$

b. $E_0 \gg \Delta$

The large E_0 case is described by the similar expansion around $E_0 \rightarrow \infty$. Introducing the triangle transformation in fig. 11 (a) with $E_{\mathbf{k}_A} \equiv \Delta/\sin \theta_A$ and $E_{\mathbf{k}_B} \equiv \Delta/\sin \theta_B$, the integral changes: $\int_{\Delta}^{\infty} dE_{\mathbf{k}_A} \int_{\Delta}^{\infty} dE_{\mathbf{k}_B} \rightarrow \int_0^{\pi/2} d\theta_A (-\Delta \cot \theta_A \csc \theta_A) \int_0^{\pi/2} d\theta_B (-\Delta \cot \theta_B \csc \theta_B)$. Rescaling the energy by Δ , we obtain

$$\begin{aligned} \mathcal{I}(E_0, \Delta) &= \int_0^{\pi/2} \int_0^{\pi/2} d\theta_A d\theta_B \frac{\csc^2 \theta_A \csc \theta_B}{\Delta(E_0^2 + (\csc \theta_A^2 + \csc \theta_B^2)^2)}, \\ &\approx \frac{1}{\Delta} \cdot \begin{cases} \int d\theta_B \cdot 1 & \text{for } \theta_B \ll 1 \\ \int d\theta_B \frac{\csc \theta_B (\pi E_0 - 2 \csc \theta_B)}{2E_0^2} & \text{for } E_0 \gg \Delta \end{cases} \end{aligned} \quad (\text{C25})$$

A crossover approximation around $\theta_B = 1/E_0$ is dealt by integrating the two approximations in eq. (C25) up

$\mathcal{O}(E_0)$:

$$\begin{aligned} \mathcal{I}(E_0, \Delta) &\approx \frac{1}{\Delta} \left(\int_0^{1/E_0} d\theta_B \right. \\ &\quad \left. + \int_{1/E_0}^{\pi/2} d\theta_B \frac{\csc \theta_B (\pi E_0 - 2 \csc \theta_B)}{2E_0^2} \right), \\ &= \frac{\pi \ln(2E_0/\Delta)}{2E_0} + \mathcal{O}((E_0/\Delta)^3), \quad \text{for } E_0 \gg \Delta. \end{aligned} \quad (\text{C26})$$

Combining eq. (C24) and eq. (C26), we obtain the double integral approximation for the double sum in eq. (C22):

$$\mathcal{I}(E_0, \Delta) = \begin{cases} \frac{\pi^2}{2\Delta} \left(1 - \frac{E_0^2}{16\Delta^2} \right), & \text{for } E_0 \ll \Delta \\ \frac{\pi \ln(2E_0/\Delta)}{2E_0}, & \text{for } E_0 \gg \Delta \end{cases}.$$

fig. 11 (b) plots the analytical solution $\mathcal{I}(E_0, \Delta)$ (solid line) and the numerical double sum (circle markers).

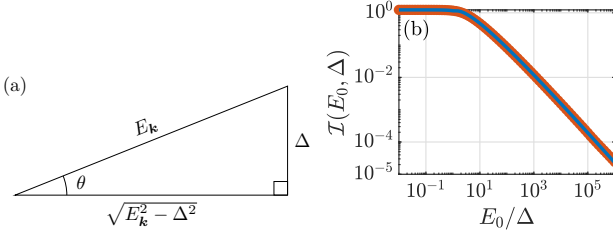


FIG. 11. (a) Triangle transformation for calculating the momentum sum in $\mathcal{I}(E_0, \Delta)$. With this transformation, we change the integral $\int_0^\infty dE_k \rightarrow \int_0^{\pi/2} d\theta (-\Delta \cot \theta \csc \theta)$. (b) Numerical (circles) and analytical approximation (solid line) of the double sum $\mathcal{I}(E_0, \Delta)$.

Appendix D: Spatial BCS Theory

The inductance of an inductor depends on its shape and the material properties. To take care of the device's geometries, we express the superconducting fermionic Hamiltonian in the spatial representation. Consider a bulk superconductor in the presence of a vector potential \mathbf{A} , the Hamiltonian is given by [26, 38]

$$H_{K_A} + H_{I_A} = \int_{SC} dV \left\{ c_{rs}^\dagger \left[\frac{1}{2m} (\mathbf{p} - e\mathbf{A}^{\text{int}})^2 - \mu \right] c_{rs} - |g|^2 c_{r\uparrow}^\dagger c_{-r\downarrow}^\dagger c_{-r\downarrow} c_{r'\uparrow} \right\}. \quad (\text{D1})$$

In the Hamiltonian, the electron momentum operator \mathbf{p} acts on the fermionic space, while the vector potential operator \mathbf{A}^{int} acts on the electromagnetic space. The fermionic field operators in the spatial representation are the Fourier's transform of those in the momentum space [26],

$$c_{rs} = \frac{1}{\sqrt{V}} \sum_{\mathbf{k}} e^{i\mathbf{k}\cdot\mathbf{r}} c_{\mathbf{k}s}. \quad (\text{D2})$$

The matter phase of the superconductor now has position dependence, so the basis state relies on the position as well. The system projector onto the low-energy subspace becomes

$$\Pi = \bigotimes_{\mathbf{r}} P_{\mathbf{r}}, \quad (\text{D3})$$

where $P_{\mathbf{r}} = \sum_{\phi(\mathbf{r})} |\Psi_{\mathbf{r}}[\phi(\mathbf{r})]\rangle \langle \Psi_{\mathbf{r}}[\phi(\mathbf{r})]|$ is the low-energy projector on the coordinate \mathbf{r} . For simplicity, we consider the quasi-1D wire model, so the projector reduces to eq. (64), depending only on the axial coordinate z . The z -dependent basis state can be expressed with the use of eq. (D2) and lemma 1:

$$|\Psi_z[\phi(z)]\rangle = \prod_{\mathbf{k}} [u_{\mathbf{k}} + v_{\mathbf{k}} (e^{i\phi(z)/2} c_{\mathbf{k}\uparrow}^\dagger) (e^{i\phi(z)/2} c_{-\mathbf{k}\downarrow}^\dagger)] |0\rangle. \quad (\text{D4})$$

The derivation is given in appendix D 1. The inclusion of the spatial-dependence gives rise to an additional

phase in fermionic field operators. After transforming the fermionic Hamiltonian eq. (1) to the spatial representation eq. (D1) and constructing the new distributed projector Π in eq. (64), we can evaluate the inductance Hamiltonian by the projection:

$$\begin{aligned} H_L &= \Pi(H_{K_A} + H_{I_A})\Pi, \\ &= \bigotimes_z P_z H P_z, \\ &= \bigotimes_z \sum_{\phi(z)\bar{\phi}(z)} \langle \Psi_z[\phi(z)] | (H_{K_A} + H_{I_A}) | \Psi_z[\bar{\phi}(z)] \rangle \\ &\quad \times |\Psi_z[\phi(z)]\rangle \langle \Psi_z[\bar{\phi}(z)]|, \\ &\approx \bigotimes_z \sum_{\phi(z)} \langle \Psi_z[\phi(z)] | (H_{K_A} + H_{I_A}) | \Psi_z[\phi(z)] \rangle \\ &\quad \times |\Psi_z[\phi(z)]\rangle \langle \Psi_z[\phi(z)]|. \end{aligned} \quad (\text{D5})$$

In the last line we apply the approximation

$$\begin{aligned} &\langle \Psi_z[\phi(z)] | (H_{K_A} + H_{I_A}) | \Psi_z[\bar{\phi}(z)] \rangle \\ &\approx \langle \Psi_z[\phi(z)] | (H_{K_A} + H_{I_A}) | \Psi_z[\phi(z)] \rangle \delta_{\phi(z), \bar{\phi}(z)}, \end{aligned}$$

according to orthogonality of BCS basis states. Namely, the off-diagonal matrix elements are negligible in the infinite limit $n \rightarrow \infty$.

For simplicity, we choose the gauge

$$\mathcal{G}_{\phi(z)} = e^{i\phi(z)\hat{N}/2}, \quad (\text{D6})$$

such that $c_{zs}^\dagger \mapsto \tilde{c}_{zs}^\dagger = e^{-i\phi(z)/2} c_{zs}^\dagger$ and $c_{zs} \mapsto \tilde{c}_{zs} = e^{i\phi(z)/2} c_{zs}$. This gauge removes the $\phi(z)$ -dependence on the bra and ket, i.e.,

$$\begin{aligned} &\langle \Psi_z[\phi(z)] | (H_{K_A} + H_{I_A}) | \Psi_z[\phi(z)] \rangle \\ &= \langle \Psi | e^{-i\phi(z)/2} (H_{K_A} + H_{I_A}) e^{i\phi(z)/2} | \Psi \rangle. \end{aligned} \quad (\text{D7})$$

In our quasi-1D model, the electron momentum operator is given by $\mathbf{p} \mapsto -i\hbar\partial_z \mathbf{e}_z$ and the vector potential $\mathbf{A}^{\text{int}} = A_z^{\text{int}} \mathbf{e}_z$. The derivative operators acting on the gauge transformed state are

$$\partial_z e^{i\phi(z)/2} c_{zs} | \Psi \rangle = e^{i\phi(z)/2} \frac{i}{2} \phi'(z) c_{zs} | \Psi \rangle, \quad (\text{D8})$$

and

$$\begin{aligned} &\partial_z^2 e^{i\phi(z)/2} c_{zs} | \Psi \rangle \\ &= e^{i\phi(z)/2} \left[\left(\frac{i}{2} \phi'(z) \right)^2 + \frac{i}{2} \phi''(z) \right] c_{zs} | \Psi \rangle. \end{aligned} \quad (\text{D9})$$

Assuming the matter phase is adiabatic, $\phi''(z) = 0$, and choosing Coulomb gauge $\nabla \cdot \mathbf{A}^{\text{int}} = 0$, eq. (D7) reduces to

$$\begin{aligned} &\langle \Psi_z[\phi(z)] | (H_{K_A} + H_{I_A}) | \Psi_z[\phi(z)] \rangle \\ &= \frac{1}{2} \frac{De^2}{m} \int_{SC} dV \left(\frac{\Phi_0}{2\pi} \phi'(z) - A_z^{\text{int}} \right)^2 + \mathcal{V}(\phi), \end{aligned} \quad (\text{D10})$$

where the electron density is defined by $D \equiv \langle \Psi | c_{zs}^\dagger c_{zs} | \Psi \rangle$ and $\varphi = \bar{\phi} - \phi$. As the projection of the interaction term gives a constant, we can choose the energy baseline to be $\Pi H_{I_A} \Pi = \mathcal{V}(\varphi) = 0$. The projection then becomes

$$\begin{aligned} \Pi H_{K_A} \Pi &\approx \bigotimes_z \sum_{\phi(z)} \frac{1}{2} \frac{De^2}{m} \int_{\text{SC}} dV \left(\frac{\Phi_0}{2\pi} \phi'(z) - A_z^{\text{int}} \right)^2 \\ &\quad \times |\Psi_z[\phi(z)]\rangle \langle \Psi_z[\phi(z)]|, \\ &= \frac{1}{2} \frac{1}{\mu_0 \lambda_L^2} \int_{\text{SC}} dV \left(\frac{\Phi_0}{2\pi} \hat{\phi}'(z) - A_z^{\text{int}}(\hat{i}_s) \right)^2, \end{aligned} \quad (\text{D11})$$

in which we re-express the factor: $\frac{De^2}{m} = \frac{1}{\mu_0 \lambda_L^2}$. Considering a cylindrical superconducting wire, the volume integral over the superconducting device is $\int_{\text{SC}} dV = \int_0^{2\pi} d\theta \int_0^l dz \int_0^{r_w} r dr$, and $A_z^{\text{int}}(\hat{i}_s)$ is given in eq. (E6). With the current operator $\hat{i}_s = \frac{\Phi_0}{2\pi} \hat{\phi}'(z)/\bar{L}$ adopted from eq. (72), and applying the lumped element approximation, $\hat{\phi}'(z) = (\hat{\phi}_B - \hat{\phi}_A)/l = -\hat{\phi}/l$, eq. (D11) becomes

$$\begin{aligned} \Pi H_{K_A} \Pi &= \frac{1}{2} \left(\frac{\Phi_0}{2\pi} \right)^2 \frac{1}{\mu_0 \lambda_L^2} 2\pi \underbrace{\int_0^l dz \hat{\phi}'^2(z)}_{=\hat{\phi}^2/l} \int_0^{r_w} r dr \left(1 - \frac{\mu_0 \lambda_L}{2\pi r_w \bar{L}} \frac{1 - I_0(r/\lambda_L)}{I_1(r_w/\lambda_L)} \right)^2, \\ &= \frac{1}{2} \left(\frac{\Phi_0}{2\pi} \right)^2 \frac{2\pi}{\mu_0 l} \frac{\hat{\phi}^2}{\lambda_L^2} \left\{ \frac{r_w^2}{2} + \frac{\mu_0 l}{2\pi L} \left[\lambda_L^2 \left(\frac{\mu_0 l}{4\pi L} \left(\frac{1 + I_0^2(r_w/\lambda_L)}{I_1^2(r_w/\lambda_L)} - 1 \right) + 2 \right) - \frac{1}{I_1(r_w/\lambda_L)} \left(r_w \lambda_L - \frac{\mu_0 l}{\pi L} \frac{\lambda_L^3}{r_w} \right) \right] \right\}, \\ &\approx \frac{1}{2} \left(\frac{\Phi_0}{2\pi} \right)^2 \hat{\phi}^2 \frac{1}{L}, \quad \text{for } \lambda_L \ll r_w, \end{aligned} \quad (\text{D12})$$

where the $I_1^{-1}(r_w/\lambda_L)$ is exponentially suppressed and $(1 + I_0^2(r_w/\lambda_L))/I_1^2(r_w/\lambda_L) \approx 1$ in the limit $r_w \gg \lambda_L$.

As the projection of the interaction $\Pi H_{I_A} \Pi$ gives a constant, the effective Hamiltonian of the superconducting inductor H_L is dominated by $\Pi H_{K_A} \Pi$. Eventually we obtain

$$H_L = \Pi(H_{K_A} + H_{I_A})\Pi \approx \frac{E_L}{2} \hat{\phi}^2, \quad (\text{D13})$$

where the inductance energy of the system E_L consists of the kinetic and geometric contributions: $E_L = (\frac{\Phi_0}{2\pi})^2/L$, where $L = L_K + L_G$.

1. Spatial-Dependent BCS State & Projections

The BCS state changes when we consider a spatial-dependent matter phase $\phi(\mathbf{r})$. Here we consider the case which the matter phase depends on all three coordinates of the space. To derive the BCS state in position representation, we require the Fourier's transform eq. (D2) and lemma 1. With the substitution $u_{\mathbf{k}} \rightarrow A_{\mathbf{k}}$, $v_{\mathbf{k}} e^{i\phi} \int d\mathbf{r}_{\mathbf{k}} \int d\mathbf{r}'_{\mathbf{k}} e^{i\mathbf{k} \cdot (\mathbf{r}_{\mathbf{k}} - \mathbf{r}'_{\mathbf{k}})} c_{\mathbf{r}_{\mathbf{k}} \uparrow}^\dagger c_{-\mathbf{r}'_{\mathbf{k}} \downarrow}^\dagger \rightarrow B_{\mathbf{k}}$, we obtain

$$\begin{aligned}
|\Psi(\phi)\rangle &= \prod_{\mathbf{k}} \left(u_{\mathbf{k}} + v_{\mathbf{k}} e^{i\phi} c_{\mathbf{k}\uparrow}^\dagger c_{-\mathbf{k}\downarrow}^\dagger \right) |0\rangle, \\
&= \prod_{\mathbf{k}} \left(u_{\mathbf{k}} + v_{\mathbf{k}} e^{i\phi} \int d\mathbf{r}_{\mathbf{k}} \int d\mathbf{r}'_{\mathbf{k}} e^{i\mathbf{k}\cdot(\mathbf{r}_{\mathbf{k}}-\mathbf{r}'_{\mathbf{k}})} c_{\mathbf{r}_{\mathbf{k}}\uparrow}^\dagger c_{-\mathbf{r}'_{\mathbf{k}}\downarrow}^\dagger \right) |0\rangle, \\
&= \sum_{m=0}^n \sum_{\chi \in \mathcal{S}_m} \prod_{\mathbf{k}_i \in \chi^c} u_{\mathbf{k}_i} \prod_{\mathbf{k}_j \in \chi} v_{\mathbf{k}_j} e^{i\phi} \int d\mathbf{r}_{\mathbf{k}_j} \int d\mathbf{r}'_{\mathbf{k}_j} e^{i\mathbf{k}_j \cdot (\mathbf{r}_{\mathbf{k}_j} - \mathbf{r}'_{\mathbf{k}_j})} c_{\mathbf{r}_{\mathbf{k}_j}\uparrow}^\dagger c_{-\mathbf{r}'_{\mathbf{k}_j}\downarrow}^\dagger |0\rangle, \\
&= \sum_{m=0}^n \sum_{\chi \in \mathcal{S}_m} \prod_{\mathbf{k}_i \in \chi^c} u_{\mathbf{k}_i} \prod_{\mathbf{k}_j \in \chi} v_{\mathbf{k}_j} \int d\mathbf{r}_{\mathbf{k}_j} \int d\mathbf{r}'_{\mathbf{k}_j} e^{i\mathbf{k}_j \cdot (\mathbf{r}_{\mathbf{k}_j} - \mathbf{r}'_{\mathbf{k}_j})} \left(e^{i\phi/2} c_{\mathbf{r}_{\mathbf{k}_j}\uparrow}^\dagger \right) \left(e^{i\phi/2} c_{-\mathbf{r}'_{\mathbf{k}_j}\downarrow}^\dagger \right) |0\rangle, \\
&\rightarrow \sum_{m=0}^n \sum_{\chi \in \mathcal{S}_m} \prod_{\mathbf{k}_i \in \chi^c} u_{\mathbf{k}_i} \prod_{\mathbf{k}_j \in \chi} v_{\mathbf{k}_j} \int d\mathbf{r}_{\mathbf{k}_j} \int d\mathbf{r}'_{\mathbf{k}_j} e^{i\mathbf{k}_j \cdot (\mathbf{r}_{\mathbf{k}_j} - \mathbf{r}'_{\mathbf{k}_j})} \left(e^{i\phi(\mathbf{r})/2} c_{\mathbf{r}_{\mathbf{k}_j}\uparrow}^\dagger \right) \left(e^{i\phi(\mathbf{r})/2} c_{-\mathbf{r}'_{\mathbf{k}_j}\downarrow}^\dagger \right) |0\rangle, \quad (\text{D14a}) \\
&= \prod_{\mathbf{k}} \left[u_{\mathbf{k}} + v_{\mathbf{k}} \left(e^{i\phi(\mathbf{r})/2} c_{\mathbf{k}\uparrow}^\dagger \right) \left(e^{i\phi(\mathbf{r})/2} c_{-\mathbf{k}\downarrow}^\dagger \right) \right] |0\rangle, \quad (\text{D14b}) \\
&\equiv |\Psi(\phi[\mathbf{r}])\rangle.
\end{aligned}$$

In Eq. D14a, we generalise the matter phase from constant to position-dependent, $\phi \rightarrow \phi(\mathbf{r})$. Hence we express the BCS ground state in spatial representation.

The additional phase terms in eq. (D14a) vanish under the gauge transformation $\mathcal{G}_{\phi(\mathbf{r})} = e^{i\phi(\mathbf{r})\hat{N}/2}$. Therefore, the

electron kinetic energy with respect to the ground state reads

$$\begin{aligned} & \left\langle \int d\mathbf{r} c_{\mathbf{rs}}^\dagger \left[\frac{1}{2m} (i\hbar\nabla - q\mathbf{A})^2 - \mu \right] c_{\mathbf{rs}} \right\rangle \\ &= \langle \Psi[\phi(\mathbf{r})] | \int d\mathbf{r} c_{\mathbf{rs}}^\dagger \left[\frac{1}{2m} (i\hbar\nabla - q\mathbf{A})^2 - \mu \right] c_{\mathbf{rs}} | \Psi[\phi(\mathbf{r})] \rangle, \end{aligned} \quad (\text{D15a})$$

$$\begin{aligned} &= \langle 0 | \sum_{m=0}^n \sum_{\chi \in \mathcal{S}_m} \prod_{\mathbf{k}_i \in \chi^c} u_{\mathbf{k}_i} \prod_{\mathbf{k}_j \in \chi} v_{\mathbf{k}_j} \int d\mathbf{r}_{\mathbf{k}_j} \int d\mathbf{r}'_{\mathbf{k}_j} e^{-i\mathbf{k}_j \cdot (\mathbf{r}_{\mathbf{k}_j} - \mathbf{r}'_{\mathbf{k}_j})} \left(e^{-i\phi(\mathbf{r})/2} c_{-\mathbf{r}_{\mathbf{k}_j}\downarrow} \right) \left(e^{-i\phi(\mathbf{r})/2} c_{\mathbf{r}'_{\mathbf{k}_j}\uparrow} \right) \\ & \quad \times \int d\mathbf{r} c_{\mathbf{rs}}^\dagger \left[\frac{1}{2m} (i\hbar\nabla - q\mathbf{A})^2 - \mu \right] c_{\mathbf{rs}} \sum_{m'=0}^n \sum_{\chi' \in \mathcal{S}'_m} \prod_{\mathbf{k}'_i \in \chi^c} u_{\mathbf{k}'_i} \prod_{\mathbf{k}'_j \in \chi} v_{\mathbf{k}'_j} \int d\mathbf{r}''_{\mathbf{k}'_j} \int d\mathbf{r}'''_{\mathbf{k}'_j} \\ & \quad \times e^{i\mathbf{k}'_j \cdot (\mathbf{r}_{\mathbf{k}'_j} - \mathbf{r}''_{\mathbf{k}'_j})} \left(e^{i\phi(\mathbf{r})/2} c_{\mathbf{r}''_{\mathbf{k}'_j}\uparrow}^\dagger \right) \left(e^{i\phi(\mathbf{r})/2} c_{-\mathbf{r}'''_{\mathbf{k}'_j}\downarrow}^\dagger \right) |0\rangle, \\ &= \langle 0 | \sum_{m=0}^n \sum_{\chi \in \mathcal{S}_m} \prod_{\mathbf{k}_i \in \chi^c} u_{\mathbf{k}_i} \prod_{\mathbf{k}_j \in \chi} v_{\mathbf{k}_j} \int d\mathbf{r}_{\mathbf{k}_j} \int d\mathbf{r}'_{\mathbf{k}_j} e^{-i\mathbf{k}_j \cdot (\mathbf{r}_{\mathbf{k}_j} - \mathbf{r}'_{\mathbf{k}_j})} \\ & \quad \times \underbrace{\mathcal{G}_{\phi(\mathbf{r})}^\dagger \mathcal{G}_{\phi(\mathbf{r})} \left(e^{-i\phi(\mathbf{r})/2} c_{-\mathbf{r}_{\mathbf{k}_j}\downarrow} \right)}_{=c_{-\mathbf{r}_{\mathbf{k}_j}\downarrow}} \underbrace{\mathcal{G}_{\phi(\mathbf{r})}^\dagger \mathcal{G}_{\phi(\mathbf{r})} \left(e^{-i\phi(\mathbf{r})/2} c_{\mathbf{r}'_{\mathbf{k}_j}\uparrow} \right)}_{=c_{\mathbf{r}'_{\mathbf{k}_j}\uparrow}} \mathcal{G}_{\phi(\mathbf{r})}^\dagger \mathcal{G}_{\phi(\mathbf{r})} \\ & \quad \times \int d\mathbf{r} \underbrace{\mathcal{G}_{\phi(\mathbf{r})}^\dagger c_{\mathbf{rs}}^\dagger \mathcal{G}_{\phi(\mathbf{r})}^\dagger}_{=e^{i\phi(\mathbf{r})/2} c_{\mathbf{rs}}^\dagger} \mathcal{G}_{\phi(\mathbf{r})} \left[\frac{1}{2m} (i\hbar\nabla - q\mathbf{A})^2 - \mu \right] \mathcal{G}_{\phi(\mathbf{r})}^\dagger \underbrace{\mathcal{G}_{\phi(\mathbf{r})} c_{\mathbf{rs}} \mathcal{G}_{\phi(\mathbf{r})}^\dagger}_{=e^{i\phi(\mathbf{r})/2} c_{\mathbf{rs}}} \mathcal{G}_{\phi(\mathbf{r})} \\ & \quad \times \sum_{m'=0}^n \sum_{\chi' \in \mathcal{S}'_m} \prod_{\mathbf{k}'_i \in \chi^c} u_{\mathbf{k}'_i} \prod_{\mathbf{k}'_j \in \chi} v_{\mathbf{k}'_j} \int d\mathbf{r}''_{\mathbf{k}'_j} \int d\mathbf{r}'''_{\mathbf{k}'_j} e^{i\mathbf{k}'_j \cdot (\mathbf{r}_{\mathbf{k}'_j} - \mathbf{r}''_{\mathbf{k}'_j})} \\ & \quad \times \underbrace{\mathcal{G}_{\phi(\mathbf{r})}^\dagger \mathcal{G}_{\phi(\mathbf{r})} \left(e^{i\phi(\mathbf{r})/2} c_{\mathbf{r}''_{\mathbf{k}'_j}\uparrow}^\dagger \right)}_{=c_{\mathbf{r}''_{\mathbf{k}'_j}\uparrow}} \underbrace{\mathcal{G}_{\phi(\mathbf{r})}^\dagger \mathcal{G}_{\phi(\mathbf{r})} \left(e^{i\phi(\mathbf{r})/2} c_{-\mathbf{r}'''_{\mathbf{k}'_j}\downarrow}^\dagger \right)}_{=c_{-\mathbf{r}'''_{\mathbf{k}'_j}\downarrow}} \mathcal{G}_{\phi(\mathbf{r})}^\dagger \mathcal{G}_{\phi(\mathbf{r})} |0\rangle, \\ &= \langle 0 | \sum_{m=0}^n \sum_{\chi \in \mathcal{S}_m} \prod_{\mathbf{k}_i \in \chi^c} u_{\mathbf{k}_i} \prod_{\mathbf{k}_j \in \chi} v_{\mathbf{k}_j} \int d\mathbf{r}_{\mathbf{k}_j} \int d\mathbf{r}'_{\mathbf{k}_j} e^{-i\mathbf{k}_j \cdot (\mathbf{r}_{\mathbf{k}_j} - \mathbf{r}'_{\mathbf{k}_j})} \mathcal{G}_{\phi(\mathbf{r})}^\dagger c_{-\mathbf{r}_{\mathbf{k}_j}\downarrow} c_{\mathbf{r}'_{\mathbf{k}_j}\uparrow} \\ & \quad \times \frac{1}{2m} \int d\mathbf{r} e^{-i\phi(\mathbf{r})/2} c_{\mathbf{rs}}^\dagger \left[(i\hbar\nabla - q\mathbf{A})^2 - \mu \right] e^{i\phi(\mathbf{r})/2} c_{\mathbf{rs}} \\ & \quad \times \sum_{m'=0}^n \sum_{\chi' \in \mathcal{S}'_m} \prod_{\mathbf{k}'_i \in \chi^c} u_{\mathbf{k}'_i} \prod_{\mathbf{k}'_j \in \chi} v_{\mathbf{k}'_j} \int d\mathbf{r}''_{\mathbf{k}'_j} \int d\mathbf{r}'''_{\mathbf{k}'_j} e^{i\mathbf{k}'_j \cdot (\mathbf{r}_{\mathbf{k}'_j} - \mathbf{r}''_{\mathbf{k}'_j})} c_{\mathbf{r}''_{\mathbf{k}'_j}\uparrow}^\dagger c_{-\mathbf{r}'''_{\mathbf{k}'_j}\downarrow}^\dagger \mathcal{G}_{\phi(\mathbf{r})} |0\rangle, \\ &= \langle \Psi(\phi=0) | \frac{1}{2m} \int d\mathbf{r} e^{-i\phi(\mathbf{r})/2} c_{\mathbf{rs}}^\dagger \left[(i\hbar\nabla - q\mathbf{A})^2 - t\mu \right] e^{i\phi(\mathbf{r})/2} c_{\mathbf{rs}} | \Psi(\phi=0) \rangle, \\ &= \langle \Psi | \frac{1}{2m} \int d\mathbf{r} e^{-i\phi(\mathbf{r})/2} c_{\mathbf{rs}}^\dagger \left[(i\hbar\nabla - q\mathbf{A})^2 - \mu \right] e^{i\phi(\mathbf{r})/2} c_{\mathbf{rs}} | \Psi \rangle. \end{aligned} \quad (\text{D15b})$$

Note that the derivative operators ∇, ∇^2 act on the position space, and the field operators $c_{\mathbf{rs}}^\dagger, c_{\mathbf{rs}}$ act on the fermionic Fock state.

Appendix E: Vector potential of a Superconducting Wire

In this appendix, we solve the London equation for a superconducting wire in a cylindrical coordinates and obtain the magnetic field inside the wire. The system can be referred to fig. 7. We then estimate the flux around the wire out to a specific distance, and calculate the geomet-

ric inductance as the magnetic field is linked to the current. In addition, we also compute the \mathbf{A}^{int} -field inside the superconductor induced by the supercurrent. This field associates to the change of the electromotive force inside the metal and gives rise to the kinetic inductance.

With Ampère's law, the London equation is expressed as $\nabla \times \nabla \times \mathbf{H}^{\text{int}} + \mathbf{H}^{\text{int}}/\lambda_L^2 = 0$, where $\mathbf{B}^{\text{int}} = \mu_0 \mathbf{H}^{\text{int}}$ and λ_L is London penetration depth. Considering a circular superconducting wire with radius r_w , we have $\mathbf{H}^{\text{int}}(r) = H_\theta(r) \mathbf{e}_\theta$ according to the cylindrical symmetry. The fields inside the metal must be finite and the boundary condition guarantees $\mathbf{H}^{\text{int}}(r = r_w) = H_0 \mathbf{e}_\theta$, so the solution reads

$$\mathbf{H}^{\text{int}}(r) = H_0 \frac{I_1(r/\lambda_L)}{I_1(r_w/\lambda_L)} \mathbf{e}_\theta, \quad (\text{E1})$$

where $I_\alpha(z)$ is the modified Bessel function of the first kind, and H_0 is the magnetic field at the surface of the cylinder. From Maxwell's equation (with zero electric field) $\nabla \times \mathbf{H}^{\text{int}} = \mathbf{J}$, the supercurrent density is along the axial direction:

$$\mathbf{J}(r) = \frac{H_0}{\lambda_L} \frac{I_0(r/\lambda_L)}{I_1(r_w/\lambda_L)} \mathbf{e}_z = J_z(r) \mathbf{e}_z. \quad (\text{E2})$$

The supercurrent \mathbf{J} in eq. (E2) is exponentially suppressed at the centre, but is not identically zero. The maximal values is at the surface $\mathbf{J}_{\text{max}} = \mathbf{J}(r_w) = \frac{H_0}{\lambda_L} \mathbf{e}_z$. The total current flowing through the wire is the surface integral over the cross section,

$$i_s = \int_{\sigma} \mathbf{J} \cdot d\sigma = 2\pi \int_0^{r_w} dr r J_z(r) = 2\pi r_w H_0, \quad (\text{E3})$$

such that the \mathbf{B}^{ext} -field outside the wire is given by

$$\mathbf{B}^{\text{ext}}(r) = \frac{\mu_0 i_s}{2\pi r} \mathbf{e}_\theta = \frac{\mu_0 r_w H_0}{r} \mathbf{e}_\theta. \quad (\text{E4})$$

The corresponding vector potential outside the metal is

$$\mathbf{A}^{\text{ext}}(r) = \frac{\mu_0 i_s}{2\pi} \ln \frac{\sqrt{l^2 + r^2} + l}{r} \mathbf{e}_z. \quad (\text{E5})$$

Gauge Invariant Vector Potential inside Superconductor We choose a gauge in which the internal vector potential is parallel to the supercurrent [24] and satisfies $\mathbf{H}^{\text{int}} = \nabla \times \mathbf{A}^{\text{int}}/\mu_0$. Solving for the current density from Maxwell's equation $\mathbf{J} = \nabla \times \nabla \times \mathbf{A}^{\text{int}}/\mu_0$, gives

$$\begin{aligned} \mathbf{A}^{\text{int}}(r) &= H_0 \mu_0 \lambda_L \frac{1 - I_0(r/\lambda_L)}{I_1(r_w/\lambda_L)} \mathbf{e}_z, \\ &= i_s \frac{\mu_0 \lambda_L}{2\pi r_w} \frac{1 - I_0(r/\lambda_L)}{I_1(r_w/\lambda_L)} \mathbf{e}_z, \\ &\approx -i_s \frac{\mu_0 \lambda_L e^{(r-r_w)/\lambda_L}}{2\pi \sqrt{r_w r}} \mathbf{e}_z \quad \text{for } \lambda_L \ll r_w. \end{aligned} \quad (\text{E6})$$

We obtain the gauge invariant vector potential inside the superconductor:

$$\tilde{\mathbf{A}}^{\text{int}}(r) = \mathbf{A}^{\text{int}}(r) + \frac{\Phi_0}{2\pi} \nabla \hat{\phi}, \quad (\text{E7})$$

where the scalar ϕ -field is self-generated by the superconductor, through changing the matter phase.

1. Classical Flux

The total inductance of the system consists of kinetic and geometric contributions. Below we compute the two terms from the viewpoint of flux.

a. Flux outside the Device

We can obtain L_G from the point of view of the induced flux Φ_{ext} , which is given by

$$\Phi_{\text{ext}} = l \int_{r_w}^R dr |\mathbf{B}^{\text{ext}}(r)| = \underbrace{\frac{\mu_0 l \ln(R/r_w)}{2\pi}}_{=L_G} \cdot i_s. \quad (\text{E8})$$

The result is consistent with the energy transfer between field and inductor.

b. Flux inside the superconductor

Here we consider the flux inside the superconductor, which gives $\Phi_{\text{int}} = i_s L_K$. By placing a superconductor in an electromagnetic field, the field penetrate the metal with a small depth, called London penetration depth λ_L . The inertia of the mobile electrons within this region is changed due to the field, and therefore gives rise to the kinetic inductance. This manifestation is similar to the change of the magnetic flux in an inductor.

2D model For the cylindrical wire model, the internal flux passing the effective surface within the wire is

$$\begin{aligned} \Phi_{\text{int}} &= \int_S \mathbf{B}^{\text{int}} \cdot d\mathbf{S}, \\ &= \frac{\mu_0 i_s l}{2\pi r_w} \frac{1}{I_1(r_w/\lambda_L)} \int_{\lambda_L}^{r_w} dr I_1(r/\lambda_L), \\ &= \frac{\mu_0 i_s l}{2\pi r_w} \frac{\lambda_L (I_0(r_w/\lambda_L) - I_0(1))}{I_1(r_w/\lambda_L)}, \\ &\approx \frac{\mu_0 i_s l \lambda_L}{2\pi r_w}, \quad \text{for } \lambda_L \ll r_w. \end{aligned} \quad (\text{E9})$$

Given London penetration depth $\lambda_L = \sqrt{m/(\mu_0 D e^2)}$ and the effective cross-section area $\sigma_{\text{eff}} \approx 2\pi r_w \lambda_L$, the Φ_{int} can be written as

$$\Phi_{\text{int}} = i_s \cdot \underbrace{\left(\frac{m}{D e^2} \frac{l}{\sigma_{\text{eff}}} \right)}_{=L_K}. \quad (\text{E10})$$

1D model Approximating the superconducting wire to a point-like wire, the internal magnetic field is given by $\mathbf{B}^{\text{int}} = \mathbf{B}^{\text{int}}(r = r_w) = \frac{\mu_0 i_s}{2\pi r_w} \mathbf{e}_\theta$, so the flux enclosed reads

$$\Phi_{\text{int}} = \int_{\sigma_{\text{eff}}} \mathbf{B}^{\text{int}} \cdot d\sigma = \frac{\mu_0 i_s l \lambda_L}{2\pi r_w} = L_K i_s. \quad (\text{E11})$$

Results in both (E12) and (E13) give the magnetic flux inside the superconducting wire, which suggests that we can link the two models by approximating the cross-section $\sigma \mapsto \sigma_{\text{eff}}$.

c. *Total Flux*

The total flux passing through a the surface from the wire up to the distance R is the sum

$$\Phi_{\text{tot}} = \Phi_{\text{int}} + \Phi_{\text{ext}} = (L_K + L_G) i_s, \quad (\text{E12})$$

which is the bias magnetic flux of the device: $\Phi_{\text{tot}} = \Phi_b$. eq. (E12) implies that the total inductance of the system is

$$L = L_K + L_G, \quad (\text{E13})$$

i.e., the inductors in series. Results eq. (E12) and eq. (E13) can be generalised to any shapes of the superconducting device.

2. Classical Energies

Here we compute the inductance from the energy and compare the results to the viewpoint of flux.

a. Energy of the Field outside the Superconductor

The electromagnetic energy stored in bmB^{ext} -field is given by

$$E_{\mathbf{B}^{\text{ext}}} = \frac{1}{2\mu_0} \int dV |\mathbf{B}^{\text{ext}}|^2 = \frac{i_s^2}{2} \frac{\mu_0 l \ln(R/r_w)}{2\pi}. \quad (\text{E14})$$

As the field can transfer energy to the inductor by the current, we obtain the geometric inductance as

$$L_G = \frac{\mu_0 l \ln(R/r_w)}{2\pi}. \quad (\text{E15})$$

b. Energies of the inside Superconductor

The energy inside the wire, including the electron kinetic energy and the field energy, contributes to the kinetic inductance.

2D model In the presence of \mathbf{A}^{int} , the kinetic energy of all electrons is described by the Hamiltonian

$$H_{\text{el}}^{(T)} = \int_{\text{SC}} dV c_{rs}^\dagger \frac{\hat{\mathbf{p}}_{\text{tot}}^2}{2m} c_{rs}, \quad (\text{E16})$$

from which we can obtain the kinetic energy with respect to the ground state by $E_{\text{el}}^{(T)} = \langle \Psi | H_{\text{el}}^{(T)} | \Psi \rangle$:

$$\begin{aligned} E_{\text{el}}^{(T)} &= \frac{m}{2D^2 e^2} \int_{\text{SC}} dV \hat{\mathbf{J}}^2 \langle \Psi | c_{rs}^\dagger c_{rs} | \Psi \rangle, \\ &= \frac{m}{De^2} \frac{H_0^2}{2\lambda_L^2 I_1^2(r_w/\lambda_L)} \cdot l \int_0^{2\pi} d\theta \int_0^{r_w} r dr I_0^2(r/\lambda_L), \\ &= \frac{i_s^2}{2} \frac{m}{De^2} \frac{l}{4\pi\lambda_L^2} \frac{I_0^2(r_w/\lambda_L) - I_1^2(r_w/\lambda_L)}{I_1^2(r_w/\lambda_L)}, \\ &\approx \frac{i_s^2}{2} \frac{m}{De^2} \frac{l}{\sigma_{\text{eff}}} \frac{1}{2}, \quad \text{for } \lambda_L \ll r_w \end{aligned} \quad (\text{E17})$$

in which we use $\sigma_{\text{eff}} \approx 2\pi r_w \lambda_L$ and adopt $H_0 = \frac{i_s}{2\pi r_w}$ from eq. (E3).

In addition to the electron kinetic energy, the other source for kinetic inductance is the energy of field inside the superconductor, $E_{\mathbf{B}^{\text{int}}}$:

$$\begin{aligned} E_{\mathbf{B}^{\text{int}}} &= \frac{1}{2\mu_0} \int_{\text{SC}} dV |E_{\mathbf{B}^{\text{int}}}|^2, \\ &= \frac{\mu_0 i_s^2 l}{8\pi r_w} \frac{1}{I_1^2(r_w/\lambda_L)} \cdot l \int_0^{2\pi} d\theta \int_0^{r_w} r dr I_1^2(r/\lambda_L), \\ &= \frac{i_s^2}{2} \frac{\mu_0 l}{4\pi r_w} \left[r_w - r_w \frac{I_0^2(r_w/\lambda_L)}{I_1^2(r_w/\lambda_L)} + 2\lambda_L \frac{I_0(r_w/\lambda_L)}{I_1(r_w/\lambda_L)} \right], \\ &\approx \frac{i_s^2 \mu_0 l \lambda_L}{2} \frac{1}{4\pi r_w}, \quad \text{for } \lambda_L \ll r_w, \\ &= \frac{i_s^2}{2} \frac{m}{De^2} \frac{l}{\sigma_{\text{eff}}} \frac{1}{2}, \quad \because \lambda_L = \sqrt{\frac{m}{\mu_0 De^2}}. \end{aligned} \quad (\text{E18})$$

The equally distributed energy in $E_{\text{el}}^{(T)}$ and $E_{\mathbf{B}^{\text{int}}}$ is the result from the equalpartition theorem in thermal equilibrium, and the sum of them gives $E_{\text{el}}^{(T)} + E_{\mathbf{B}^{\text{int}}} = \frac{1}{2} L_K i_s^2$. Therefore the kinetic inductance is given by

$$L_K = \frac{m}{De^2} \frac{l}{\sigma_{\text{eff}}}. \quad (\text{E19})$$

1D model On the other hand, the 1D wire carries a constant supercurrent density $\mathbf{J} = H_0/\lambda_L = i_s/(2\pi r_w \lambda_L)$, and the wire has the volume of $\sigma_{\text{eff}} = 2\pi r_w \lambda_L l$. Following the same procedures above, the kinetic energy of the electrons is given by

$$E_{\text{el}}^{(T)} = \frac{i_s^2}{2} \underbrace{\frac{m}{De^2} \frac{l}{\sigma_{\text{eff}}}}_{=L_K}, \quad (\text{E20})$$

which is twice of that of the 2D wire. Since the vector potential inside the quasi-1D wire is a constant, the magnetic field, which is the curl of the vector potential, is zero. Namely, the field energy inside the 1D superconducting wire is zero as well. Hence the only contribution to the kinetic inductance comes from the electrons.

c. *Total Energy*

The total energy of the system is the summation of the field energy eq. (E14) and the electron kinetic energy

eq. (E20):

$$E_{\text{tot}} = E_{\mathbf{B}^{\text{ext}}} + E_{\text{el}}^{(T)} + E_{\mathbf{B}^{\text{int}}} = \frac{i_s^2}{2} \underbrace{(L_G + L_K)}_{\equiv L}, \quad (\text{E21})$$

from which we show that the total inductance of the system as $L = L_G + L_K$. The relation provides an evidence that the total inductance of the circuit has to cover both geometric design and the material properties of the superconducting device.

[1] M. H. Devoret and R. J. Schoelkopf, *Science* **339**, 1169 (2013).

[2] J. Clarke and F. K. Wilhelm, *Nature* **453**, 1031 (2008).

[3] M. Bocko, A. Herr, and M. Feldman, *IEEE Transactions on Applied Superconductivity* **7**, 3638 (1997).

[4] A. Blais, R.-S. Huang, A. Wallraff, S. M. Girvin, and R. J. Schoelkopf, *Phys. Rev. A* **69**, 062320 (2004).

[5] G. Burkard, R. H. Koch, and D. P. DiVincenzo, *Phys. Rev. B* **69**, 064503 (2004).

[6] A. Osborne, T. Larson, S. G. Jones, R. W. Simmonds, A. Gynen, and A. Lucas, *PRX Quantum* **5**, 020309 (2024).

[7] G. Milburn, *Physics World* **16**, 24 (2003).

[8] Y. Yamamoto and A. Imamoglu, *Mesoscopic Quantum Optics* (John Wiley and Sons, 1999).

[9] T. M. Stace, C. H. W. Barnes, and G. J. Milburn, *Phys. Rev. Lett.* **93**, 126804 (2004).

[10] T. Kuhn, B. Sothmann, and J. Cayao, *Phys. Rev. B* **109**, 134517 (2024).

[11] L. I. Glazman and G. Catelani, *SciPost Phys. Lect. Notes*, **31** (2021).

[12] D. Thanh Le, J. H. Cole, and T. M. Stace, *Phys. Rev. Res.* **2**, 013245 (2020).

[13] J. Bardeen, L. N. Cooper, and J. R. Schrieffer, *Phys. Rev.* **108**, 1175 (1957).

[14] V. Bouchiat, D. Vion, P. Joyez, D. Esteve, and M. H. Devoret, *Physica Scripta* **1998**, 165 (1998).

[15] J. Annett, *Superconductivity, Superfluids and Condensates*, Oxford Master Series in Physics (OUP Oxford, 2004).

[16] D. T. Pegg and S. M. Barnett, *Phys. Rev. A* **39**, 1665 (1989).

[17] F. Mila and K. P. Schmidt, Strong-coupling expansion and effective hamiltonians, in *Introduction to Frustrated Magnetism: Materials, Experiments*, edited by C. Lacroix, P. Mendels, and F. Mila (Springer Berlin Heidelberg, Berlin, Heidelberg, 2011) pp. 537–559.

[18] O. Gunnarsson, *Rev. Mod. Phys.* **69**, 575 (1997).

[19] A. Potočnik, A. Krajnc, P. Jeglič, Y. Takabayashi, A. Y. Ganin, K. Prassides, M. J. Rosseinsky, and D. Arčon, *Scientific Reports* **4**, 4265 (2014).

[20] G. D. Mahan, *Many-particle physics / Gerald D. Mahan* (Plenum Press New York, 1981).

[21] H. Bruus, K. Flensberg, and Ø. Flensberg, *Many-Body Quantum Theory in Condensed Matter Physics: An Introduction* (Oxford Graduate Texts (OUP Oxford, 2004).

[22] W. C. Smith, A. Kou, X. Xiao, U. Vool, and M. H. Devoret, *npj Quantum Information* **6**, 8 (2020).

[23] J. D. Jackson, *Classical electrodynamics*, 3rd ed. (Wiley, New York, NY, 1999).

[24] M. Tinkham, *Introduction to Superconductivity (2nd Edition)* (Dover Publications, 1996).

[25] J. B. Ketterson and S. N. Song, *Superconductivity* (Cambridge University Press, 1999).

[26] P. Coleman, *Introduction to Many-Body Physics* (Cambridge University Press, 2015).

[27] R.-P. Riwar and D. P. DiVincenzo, *npj Quantum Information* **8**, 36 (2022).

[28] M. Peruzzo, F. Hassani, G. Szep, A. Trioni, E. Redchenko, M. Žemlička, and J. M. Fink, *PRX Quantum* **2**, 040341 (2021).

[29] J. Koch, T. M. Yu, J. Gambetta, A. A. Houck, D. I. Schuster, J. Majer, A. Blais, M. H. Devoret, S. M. Girvin, and R. J. Schoelkopf, *Phys. Rev. A* **76**, 042319 (2007).

[30] S. Corlevi (2006).

[31] J. Kadlec and K. Gundlach, *Solid State Communications* **16**, 621 (1975).

[32] T. Aref, A. Averin, S. van Dijken, A. Ferring, M. Koberidze, V. F. Maisi, H. Q. Nguyen, R. M. Nieminen, J. P. Pekola, and L. D. Yao, *Journal of Applied Physics* **116**, 073702 (2014).

[33] A. M. Goodman, *Journal of Applied Physics* **41**, 2176 (2003).

[34] K. Yang and D. F. Agterberg, *Phys. Rev. Lett.* **84**, 4970 (2000).

[35] TheTryLe, A. Grimsmo, C. Müller, and T. M. Stace, *Phys. Rev. A* **100**, 062321 (2019).

[36] C. Flamant, *Ph 295b, many-body physics: Set 5* (2016).

[37] S. Uchino, *Phys. Rev. Res.* **3**, 043058 (2021).

[38] L. P. Gor'kov, *Soviet Physics Journal of Experimental and Theoretical Physics* **7**, 505 (1958).